FINAL REPORT

CONTRACT NO.: DAMD17-91-C-1096

TITLE: Vasopressin Receptor Signaling and Cycling of Water Channels in Renal Epithelia

PRINCIPAL INVESTIGATOR: Dr. Abdul J. Mia
CO-PRINCIPAL INVESTIGATOR: Dr. Thomas Yorio

PI ADDRESS:
Division of Science and Mathematics
Jarvis Christian College
Highway 80
Hawkins, Texas 75765

REPORT DATE: August 31, 1994

TYPE OF REPORT: FINAL REPORT

PREPARED FOR:
U.S. ARMY MEDICAL RESEARCH AND
MATERIAL COMMAND
FORT DETRICK
FREDERICK, MARYLAND 21702-5012

DISTRIBUTION STATEMENT: Approved for public release; distribution unlimited.

REPORT DOCUMENTATION PAGE

Form Approved
OMB No. 0704-0188

1. AGENCY USE ONLY *(Leave blank)*	2. REPORT DATE	3. REPORT TYPE AND DATES COVERED
	08/31/94	Final 08/01/91 - 07/31/94

4. TITLE AND SUBTITLE
Vasopressin Receptor Signaling and Cycling of Water Channels in Renal Epithelia

5. FUNDING NUMBERS
DAMD17-91-C-1096
0601102A
3M161102B515 515/CA
DA 335934

6. AUTHOR(S)
Dr. A. J. Mia
Dr. T. Yorio*

7. PERFORMING ORGANIZATION NAME(S) AND ADDRESS(ES)
Jarvis Christian College
Highway 80, Hawkins, Texas 75765

8. PERFORMING ORGANIZATION REPORT NUMBER

9. SPONSORING/MONITORING AGENCY NAME(S) AND ADDRESS(ES)
U.S. Army Medical Research & Development Command
Fort Detrick
Frederick, Maryland 21702-5012

10. SPONSORING/MONITORING AGENCY REPORT NUMBER

11. SUPPLEMENTARY NOTES
*Department of Pharmacology
University of North Texas Health Science Center at Fort Worth
Fort Worth, Texas 76107

12a. DISTRIBUTION/AVAILABILITY STATEMENT
Approved for public release; distribution unlimited

12b. DISTRIBUTION CODE

13. ABSTRACT *(Maximum 200 words)*

Water reabsorption and urinary volume regulation are important processes in maintaining normal physiological function. Vasopressin (ADH) is the hormone that is responsible for regulating water homeostasis and enhancing water reabsorption during dehydration. This process is particularly important to soldiers who are subject to excess heat and fluid deprivation in arid environments. We have been examining the mechanisms whereby ADH enhances water permeability in renal epithelia so we may find measures to enhance the kidney's responsiveness to ADH. Such regimens would maintain the water reabsorptive capacity of soldiers facing harsh conditions. Our observations suggest that an integral component of the water reabsorptive process by ADH is the enzyme, protein kinase C (PKC) and calcium mobilization in addition to ADH's well established actions on cyclic AMP. Using immunocytochemical and fluorescent techniques we have identified PKC isozymes that translocate from the cytosol to the membrane during activation by ADH or PKC activators. We also have developed in vitro cultured cell model that responds to vasopressin that could be used to study transepithelial fluid and electrolyte transport and have evaluated various cultured cell filter suports for their transport characteristic limitations.

14. SUBJECT TERMS
Transepithelial water flow; Vasopressin; cultured kidney cells; Protein Kinase C; filter supports for cultured cells, RA3

15. NUMBER OF PAGES

16. PRICE CODE

17. SECURITY CLASSIFICATION OF REPORT	18. SECURITY CLASSIFICATION OF THIS PAGE	19. SECURITY CLASSIFICATION OF ABSTRACT	20. LIMITATION OF ABSTRACT
Unclassified	Unclassified	Unclassified	Unclassified

FOREWORD

Opinions, interpretations, conclusions and recommendations are those of the author and are not necessarily endorsed by the US Army.

__X__ Where copyrighted material is quoted, permission has been obtained to use such material.

__X__ Where material from documents designated for limited distribution is quoted, permission has been obtained to use the material.

__X__ Citations of commercial organizations and trade names is this report do not constitute an official Department of Army endorsement or approval of the products or services of these organizations.

__X__ In conducting research using animals, the investigator(s) adhered to the "Guide for the Care and Use of Laboratory Animals," prepared by the Committee on Care and Use of Laboratory Animals of the Institute of Laboratory Resources, National Research Council (NIH Publication No. 86-23, Revised 1985).

__N/A__ For the protection of human subjects, the investigator(s) adhered to policies of applicable Federal Law 45 CFR 46.

__N/A__ In conducting research utilizing recombinant DNA technology, the investigator(s) adhered to current guidelines promulgated by the National Institutes of Health.

__N/A__ In the conduct of research utilizing recombinant DNA, the investigator(s) adhered to the NIH Guidelines for Research Involving Recombinant DNA Molecules.

__N/A__ In the conduct of research involving hazardous organisms, the investigator(s) adhered to the CDC-NIH Guide for Biosafety in Microbiological and Biomedical Laboratories.

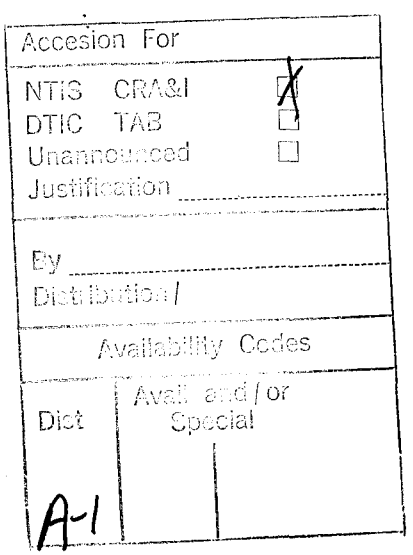

08/30/94

PI - Signature Date

TABLE OF CONTENTS

ORIGINAL FIGURE PLATES INCLUDED: 24

Vasopressin Receptor Signaling and Cycling of Water Channels in Renal Epithelia

INTRODUCTION

Eukaryotic cells in higher vertebrates evolved to perform a variety of complex molecular and cellular functions to maintain electrolyte balance and body homeostasis. In the case of kidney, the distal renal cortical and collecting tubule cells have the capacity to reabsorb fluid from the external environment into the systemic circulation to prevent dehydration, at times of thirst. This process is governed by antidiuretic hormone (ADH, vasopressin), which is designed specifically to promote rapid transmembrane water flow, across the renal epithelia under an osmotic gradient. Vasopressin is also known to exert similar stimulatory effects on fluid transport in other renal model epithelia. A tissue that has been extensively utilized as a dynamic renal membrane model for studies of transcellular fluid transport is the amphibian urinary bladder (Bentley, 1958; DiBona et al., 1969; Hays, 1983; Mia et al., 1983, 1987, 1991a and others). ADH stimulates water reabsorption in this tissue similarly to that seen in the mammalian kidney. In the present study this model epithelium was used to investigate the cellular actions of ADH.

Vasopressin mediated osmotic water transfer in renal epithelia is regulated by two receptor subtypes, V_1 and V_2, which are known to be present on the basal (serosal) plasma membrane side of the principal (granular) cells. The process whereby ADH, through its receptors, changes membrane permeability, and the molecular and cellular events leading to a rapid osmotic water flow across the apical (mucosal) membrane, are not fully understood. A schematic presentation is presented in Figure 1 to describe the relative biochemical and cellular events that occur in the unstimulated control and in

the ADH stimulated V_2 and V_1 receptor cascades in toad urinary bladder epithelial cells. These mechanisms appear to be important to water channel processes of exo- and endocytosis. The stimulation of vasopressin V_2 receptors is linked to the activation of adenylate cyclase through G proteins, which results in enhanced formation of cAMP and the activation of protein kinase A (PKA) (Handler and Orloff, 1973, 1981; Schlondorff and Levine, 1985). These biochemical events are associated with the process of water channel fusion, and is often called the exocytosis portion of enhanced water reabsorption. Such changes are also believed to be accompanied by subcellular alterations involving propagation of numerous microvilli on the exposed mucosal membrane that form out of a continuous phase of microridges (Davis et al., 1974; DiBona, 1978, 1981; Dratwa et al., 1979; Mills and Malick, 1978; Mia et al., 1983, 1988a; Spinelli et al., 1975 and others). These morphologic manifestations at the apical membrane surface of toad urinary bladder granular cells occur simultaneously with the insertion of water channels (aggrephores) at the apical membrane resulting in enhanced permeability to water. These fusion events seen in freeze-fracture replicas, appear as intramembrane particle aggregates with stellar configurations, (Chevalier et al., 1974; Gronowiez et al., 1980; Hays et al., 1985; Kachadorian et al., 1978; Mia et al., 1989; Wade et al., 1981 and others). What controls and regulates apical membrane fusion events is uncertain. The translocation of water channels or aggrephores, through the cytoplasm to the apical cell surface for fusion, is thought to be directed by dynamic actions of the microtubules and microfilaments (Hays et al., 1982; Taylor et al., 1973; Hardy and DiBona, 1982; Pearl and Taylor, 1983; Mia et al., 1991a). The molecular mechanisms involving the stimulation of the microtubule and microfilament action for the transport process of the water channels (aggrephores) are not quite understood. To further characterize these relationships, we investigated hormone actions using cultured

amphibian kidney cortical A6 cells. It was found that the effects of ADH on biochemical parameters correlated with the induction of numerous microvilli from the normal stage of microridges that predominate over the surface of control A6 cells, very similar to that reported for toad urinary bladder granular cells (Mia et al., 1988a). These kidney cortical cells grown on filter supports quickly form a confluent monolayer with tight junction suitable for electrolyte transport studies (Perkins and Handler, 1981; Candia et al., 1993).

Vasopressin also increases intracellular calcium and this effect appears to be associated with the ADH V_1 receptors coupled to phosphoinositide metabolism. The cleavage of this membrane lipid through phospholipase C (PLC) results in the propagation of myo-inositol trisphosphate (IP_3) and diacylglycerol. The IP_3 causes mobilization of intracellular calcium, whereas diacylglycerol activates the phospholipid-dependent enzyme, protein kinase C (PKC) (Ausiello et al., 1987). It is known that amphibian urinary bladder epithelia contain a vasopressin V_1 receptor coupled to phosphoinositide metabolism, with vasopressin acting to stimulate release of inositol phosphates (Schlondorff and Satriano, 1985; Yorio and Satumtira, 1989). It is not known whether the vasopressin V_1 receptor has any role in the augmentation of transmembrane water flow or regulating apical membrane fusion of water channels. Indeed our recent experimental evidence indicates that the vasopressin V_1 receptor cascade may play an integral role in the insertion of putative water channels into the apical membrane, possibly in association with the activation of PKC. Mezerein (MZ), a non-phorbol activator of PKC, when added to the mucosal surface, stimulates transmembrane osmotic water flow across the amphibian urinary bladder in a process mimicking the actions of vasopressin (Yorio and Satumtira, 1989). In addition, scanning electron microscopic studies of the surface of toad urinary bladders, treated

with MZ, revealed the induction of numerous prominent microvilli over the apical plasma membrane surface (Mia et al., 1989a, b), very similar to what was observed following challenges of toad urinary bladders with ADH. Immunogold antibody localization studies of the toad urinary bladder tissues, following stimulation with ADH and MZ, indicated localization of gold particles with cytosolic diffused bodies, as well as on apical membranes of the granular cells. Our western blot analysis of PKC isozyme I indicated the occurrence of PKC in the dissociated isolated toad urinary bladder epithelial cells. These observations suggested that both V_2 and V_1 receptors could participate in the overall scheme of enhanced water flow following hormone stimulation, particularly with regard to the increased permeability of water that occurs at the apical membrane of the granular cells. However, the relationship between V_1 receptor stimulation and PKC activation must be investigated and correlated with biochemical events to fully resolve the relative contributions of each receptor subtype to the phenomenon of osmotic water transport mediated by vasopressin.

It has been reported that PKC isozymes upon activation, are translocated from the cytosol to the apical membrane surface in several tissue types. Using FITC immunofluorescent antibody labeling techniques, PKC translocation has been demonstrated in MDBK renal epithelia (Simboli-Campbell et al., 1993), oligodendrocytes (Asotra and Mackin, 1993), human megakaryoblastic leukemic cells (Ito et al., 1988), and in cardiac myocytes and fibroblasts (Mochly-Rosen et al., 1990). Studies using the fluorescent microscopy and immunoantibody labeling techniques may be useful in determining the possible role of PKC isozyme subtypes in the translocation process of water channels from cytosol to the apical membrane. Therefore, experiments were conducted to correlate our previous morphometric studies of the toad urinary bladder tissues with translocation of water channels during enhanced water flow

mediated by ADH or activation of PKC by MZ, a chemical component known to mimic diacylglycerol to activate PKC. Our present studies use the techniques of SEM, TEM, and freeze-fracture combined with immunogold localization of PKC subtypes I, II and III in toad urinary bladder granular epithelia and cultured cells. These studies would help assess the contributions of V_1 receptor stimulation in association with PKC activation during exocytosis and transmembrane osmotic water flow. Furthermore, we also examined the role of PKC during endocytosis following withdrawal of hormonal actions and dissipation of osmotic water flow.

The process of exocytosis as it relates to the insertion of water channels into the apical membrane during osmotic water flow is reversed following hormone removal to ensure recovery of water channels into the cytoplasm for availability as a recycling process using endocytotic mechanisms to accomplish this goal. The coordinated mechanisms of exo- and endocytosis in renal and in amphibian model epithelia, as induced by ADH, has not been resolved (Coleman et al., 1987; Harris et al., 1986). Therefore, studies were carried out to examine what conditions which promote endocytosis had on water flow and morphology in toad urinary bladder sacs (Mia et al., 1993a,b,c, 1994). In addition, the role of PKC in the process of endocytosis in toad urinary bladder epithelia was carried out to determine if PKC had any role in the process of membrane retrieval. Our preliminary studies indicated that PKC may have a functional role in the process of endocytosis (Mia et al., 1994).

MATERIALS

Reagents and Antibodies:

Most reagents and immunochemicals for experimental use were obtained from the following sources: Monoclonal antibodies of protein kinase C (PKC) isozymes I(γ),

II (β), and III (α) anti-rabbit IgG, purified from rabbit brain, were purchased from Seikagaku America, Inc. Protein kinase C enzymes used as antigens for isozymes γ, β, and α, were IgG fractions from rabbit with less than 0.1% cross-reactivity with one another and were purchased from Calbiochem. Affinity purified fluorescein anti-rabbit IgG (H & L) with no free fluorescein and rabbit serum for fluorescent microscopy were purchased from Vector Laboratories. Gold particles with a diameter of 5, 10 and 20nm, conjugated to protein A-gold IgG complex and detectable as electron-opaque granules, were obtained from EY Laboratories and Sigma Chemical Co., St. Louis, MO. Aqueous 8% glutaraldehyde, aqueous 4% osmium tetroxide and L.R. White (medium) resin were purchased from Polysciences, Inc. PKC isozyme enzymes, antibodies and protein A-gold probes were diluted at a concentration between 1/15 and 1/25 using 0.1% BSA in normal Ringer's solution (Mia et al., 1992) for use. 8-arginine vasopressin and mezerein were purchased from Sigma Chemical Co., St. Louis, MO.

METHODS

Experimental Tissues:

Tropical toads, *Bufo marinus,* purchased from Carolina Biological Supply Company, Burlington, NC, were maintained at 23° C in an aquatic environment system irrigated with running tap water and were fed live crickets biweekly. Toad urinary bladder epithelial cells, freshly dissociated and collected under sterile conditions, were grown in culture media in the tissue culture incubator in a 5% CO_2 environment at 28°C. In addition, A6 toad kidney cortical cells and LLC-PK_1 cells, obtained from American Type Culture Collection (Rockville, MD) were grown similarly in the incubator at 28° C and 37°C respectively, for comparative experimental studies to evaluate the potential use of these tissues for transmembrane water flow studies.

EXPERIMENTAL PROTOCOL

Whole Bladder Sacs:

Each experimental urinary hemibladder sac was surgically removed from doubly pithed toads. Each urinary bladder sac was then suspended at the end of a glass tube as shown in Figure 2 and equilibrated for 30 min in aerated normal Ringer's solution as described previously (Bentley, 1958; Mia et al., 1983, 1987, 1991a). The Ringer's solution was composed of (in millimoles per liter): NaCl, 111; KCl, 3.35; $CaCl_2$, 2.7; MgCl, 0.5; $NaHCO_3$, 4.0 and glucose, 5.0 with pH adjusted at 8.0 by continuous aeration of the buffer solution. Hemibladder sacs from each animal were used as control and experimental tissues, and an osmotic gradient was established prior to any experimental procedure with a 1/10 dilution of mucosal Ringer's solution. Antidiuretic hormone, arginine 8-vasopressin, at a concentration of 10mU/ml or 100mU/ml was added to the serosal bath, while mezerein, at concentrations between 10^{-6} M and 10^{-9} M were added to the urinary sac (mucosal side). The MZ was dissolved in a stock solution of DMSO at a concentration of 0.05 M. The concentration of DMSO added was < 0.002%. Control and experimental tissues received identical treatments for 5, 10, 15, 20, 30, or 60 min prior to tissue fixation (Mia et al., 1991a, 1992, 1993a, b, c, 1994). At the conclusion of each experiment, sacs were withdrawn from the experimental solution, cut, emptied and dropped into 2% glutaraldehyde in PIPES (0.02M) at a pH of 7.2. This fixative was then replaced with fresh glutaraldehyde solution and fixation was allowed to continue for 1 hr. Following fixation and buffer rinses, each hemibladder sac was cut into four individual segments, with each segment reserved for SEM, TEM, freeze fracture and immunogold antibody labeling. Tissues retained for SEM and TEM received postfixation in 1% osmium tetroxide for 1 hr, but the tissues for freeze fracture replica preparations and immunogold labeling received

no postfixation with osmium tetroxide. This was particularly important to prevent possible loss of antigenic sites for immunogold antibody labeling.

Cell Culture:

Toad urinary bladder epithelial cells were dissociated and collected under sterile conditions according to procedures described previously (Yorio et al., 1983; Yorio and Satumtira, 1989; Mia et al., 1988a). During isolation procedures, all media contained antibiotics. These cells were washed and resuspended in Ca^{2+}- and Mg^{2+} -free media and transferred to Falcon flasks and petri dishes containing microscope glass cover slips for growth and confluence. The culture flasks or petri dishes containing supplemented Quimby amphibian culture media (Gibco) were retained in an incubator at 28^{0}C in 5% CO_2 environment. The culture media was changed three times/week and only primary confluent cultures were used. The toad urinary bladder granular and A6 amphibian kidney cells, upon transfer to Anocell or ICN filter supports or to glass cover slips, form confluent monolayers and tight cellular junctions. These tissues were being utilized in SEM studies and in immunofluorescent detection of PKC isozyme subtypes. For LLC-PK_1 cells, Dulbecco's Modified Eagles Medium (DMEU) was used and cells were incubated at 38^{0}C.

Scanning and Transmission Electron Microscopy (SEM, TEM):

For SEM preparations, glutaraldehyde fixed and post-osmicated tissue samples were processed through exchanges of ethanol and amyl acetate for critical point drying in liquid CO_2 in a Polaron drying apparatus. Additional critical point drying was made using Peldri II, for which tissues were dehydrated through graded acetone to transfer to liquified Peldri II for infiltration and was allowed to solidify by gradually dropping

the temperature below 23^{0}C. Peldri II was then allowed to sublimate for critical point drying using a freeze dryer or running fumehood. The dried specimens, mounted on clean aluminum stubs with silver paint, were gold coated in an argon environment using a Sputter Coater (Mia et al., 1983, 1988a). These specimens were examined in an ETEC Autoscan electron microscope operating at 20 KV, and photomicrographs were taken under similar magnifications for comparative studies. Post-osmicated tissue samples retained for TEM studies were processed through exchanges of graded ethanol and propylene oxide, for casting into individual blocks in Luft's epon resin. Polymerization was allowed to progress overnight at 60° C in an oven. Ultrathin sections prepared with a diamond knife were collected on bare nickel grids, which upon drying, were exposed to uranyl acetate and lead citrate for viewing in the TEM.

Morphometric Determination of Apical Surface Changes:

For morphometric quantitation, between four and six pictures for each treatment were taken at 1500X and 4000X magnifications using SEM. The total number of normal and treated cells in each picture image was counted and averaged to show results in percentages. The statistical analysis of each treatment group (control versus ADH and MZ) was made on a Texas Instruments Professional Computer using the Trajectories statistical program (DBI Software, Mount Pleasant, MI). The ANOVA and Fischer's PLSD (Protected Least Significant Difference) were performed with Stateview (Abacus Concepts, Inc., Berkeley, CA) on an Apple MacIntosh IIsi microcomputer. Descriptive statistical data were calculated using between 4 and 6 images, and the results presented are as mean $\pm$ 1 standard deviation. Statistical analysis of the data involving gold particles for PKC isozymes was also made using the same methods.

Immuno-Gold Cytochemistry:

For immuno-gold localization of PKC isozyme subtypes, glutaraldehyde fixed tissue samples were dehydrated and processed through exchanges of graded ethanol and L.R. White and embedded in pure L.R. White resin using gelatin capsules. Tissue blocks were allowed to polymerize in closed gelatin capsules for 15 hrs at 60° C in a vacuum oven (Mia et al., 1991a, 1992). Ultrathin sections made with a diamond knife, were collected on bare nickel grids for PKC antibody and immunogold labeling. Ultrathin sections were exposed separately to PKC antibodies I, II and III isozymes, anti-rabbit IgG and then to protein A or G-gold probes (dilution 1/15 or 1/25 using 0.1% BSA in Ringer's solution) for labeling. Each grid was exposed to a drop of monoclonal antibody for 2 hrs, and then washed and labeled with protein A-gold probes (5, 10 or 20nm) for an additional 2 hrs. Control grids received treatment with antibody or 0.1% BSA and protein A-gold probes. Labeling was carried out in a moist chamber at room temperature. For localization of two isozymes subtypes I and II in single grids, each grid was first exposed to antibody subtype II and 5nm protein A-gold probe, followed by exposure to the second subtype I antibody and 20nm protein A-gold probe. A 2 hr treatment period for each step was allowed followed by buffer rinses between treatments. Air dried grids were exposed to uranyl acetate and lead citrate for staining prior to TEM observations (Mia et al., 1991a, 1992).

Immunofluorescent Cytochemistry Using FITC:

For immunofluorescent microscopy, glass cover slips containing confluent monolayer cells were removed from culture media, rinsed 2X and were then placed in isotonic Ringer's solution for performing experimental procedures. Several cover slips were maintained in the isotonic Ringer's solution for control tissues, while other cover

slips were exposed to ADH 100 mU/ml or MZ10^{-6}M for 15 min for stimulation prior to fixation. Control and experimental culture cells were then fixed in 3% formaldehyde in PBS buffer for 1 hr, and then rendered permeable by plunging in cold methanol (Yorio et al., 1985). After 10 min in methanol, the permeabilized cells were rinsed in PBS buffer, and then exposed to PKC antibody isozymes (1/15 dilution) for 1 to 2 hr at room temperature in a moist chamber. Tissues received a thorough wash in the same buffer, were treated with anti-body IgG conjugated with fluorescein isothiocyanate (FITC; 1/16 dilution) for 2 hr in the dark at room temperature. Cells were washed in PBS buffer and deionized water to mount on medium containing 9:1 glycerol and PBS buffer. Control cells received treatment only with 0.1% BSA and fluorescein isothiocyanate (FITC). The preparations were examined in a Nikon Optiphot fluorescent microscope equipped with a narrow epifluorescent barrier filter. Photomicrographs were recorded on Kodak Tri-X film ASA 400 and developed in a solution of Microdol-X developer.

Freeze Fracture Replica Preparation:

For freeze fracture, small pieces of cryoprotected (in 30% glycerol) tissue samples were placed on standard copper holders and then plunged into liquid freon cooled to -190° C in a liquid nitrogen bath. Freeze fracture was performed in a Balzers 400T apparatus at -100° C with a metal knife cooled with liquid nitrogen. The fractured surfaces were shadowed with evaporated platinum at an angle of 35°, and then coated with evaporated carbon at a 90° angle. Some freeze fractured tissues were allowed to etch for 5 or 10 min to reveal detailed microstructures. The replicas upon removal from the freeze fracture apparatus were quickly coated with 1% collodion in amyl acetate while still frozen. Collodion coated replicas were placed in 5.25% Na

hypochlorite solution which was adequate for tissue digestion, and later washed and placed on bare copper grids for TEM studies.

PKC Assay Using Cultured Epithelial Cells:

A rapid simple protein kinase C (PKC) assay based on a mixed micelle method that can be routinely performed using tissue culture cells was developed by our laboratory (Cammarata et al., 1993). Enzyme preparation was performed in membrane and cytosolic fractions respectively. The isolation of these fractions followed the sequence listed below.

PKC Determination:

Cultured A6 cells were washed in serum-free medium. Cells were exposed to Ca^{2+}-and Mg^{2+}-free PBS containing 0.25% trypsin + 1 mM EGTA for 5 min. Isolated cells were collected and resuspended in serum-containing or serum-free media. Cells were incubated with hormone and/or drugs for a predetermined time. The incubation was stopped by adding five-fold cold media and the cells were quickly centrifuged. Collected A6 cells were homogenized in 2 ml of buffer (A) containing 20 mM Tris-HCl, pH 7.5; 0.5 mM EGTA; and 25 μg/ml each of apotinin and leupeptin. Homogenate was centrifuged at 100,000 xg at 4° C for 30 min, yielding a soluble (cytosolic) and particulate (membrane) fraction. The enzyme in the membrane fraction was solubilized in 2 ml of buffer (A) supplemented with 0.5% Triton X-100 and homogenized. The homogenate was incubated on ice for 30 min, followed by centrifugation at 100,000 xg for 30 min. The soluble and membrane-bound extracted enzymes were partially purified by chromatography on DEAE-cellulose (DE52) after elution with 200 mM NaCl. The eluate from the DE52 column containing enzyme was

desalted by chromatography on Sephadex G25 and eluted with 20mM Tris-HCl. The eluted soluble enzyme or membrane-bound extracted enzyme from the Sephadex G25 column was used for subsequent PKC analysis.

The PKC activity was followed by phosphorylation of its substrate (AC-MBP 4-14, a PKC substrate peptide purchased from Gibco) using ^{32}P-ATP measured at 30^0 C in an incubation volume of 50ul for 5 min. The assay mixture contained in final concentration: ATP, 20μM; $MgCl_2$, 10mM; $CaCl_2$, 200 μM; substrate, 25 μM; phosphatidyl serine, 516 μM; 1-oleoyl-2-acetylglycerol (OAG), 344 μM; enzyme, 5-15 μg; Tris-HCl, 20 mM, pH = 7.5, with or without 20 μM substrate-specific PKC inhibitor (PKC inhibitor peptide 19-36 from Gibco). About 500,000 cpm of ^{32}P-ATP was added to each test tube. The reaction was started by addition of ATP and stopped by taking 25μl of assay mixture and spotting onto phosphocellulose paper. Free ^{32}P-ATP and ^{32}-labelled substrate were separated by washing the paper with 0.85% of phosphoric acid for 5 min twice, followed by another two washes with distilled water. The radioactivity retained on the phosphocellulose paper after washing was determined by counting the paper in 10ml of scintillation liquid. PKC activity was determined by the difference between the activities in the absence and presence of the PKC substrate inhibitor. A unit of PKC activity was defined as incorporation of 1 μmol of phosphate into the substrate per min per mg protein. Proteins were determined using the method of Bradford (1976).

Transepithelial Water Flow Measurements of A6 Cells Grown on Filter Supports:

The morphological SEM observations suggested that A6 cells responded to both hormone and MZ, a PKC activator in a similar fashion. To determine if these changes were associated with increases in membrane permeability and enhanced water

transport, osmotic water flow was measured across A6 cells grown to confluency on Anocell or ICN Cellagen filter supports. Although there was an apparent morphological change following hormone addition, and previous data had shown an increase in adenylate cyclase activity, there was no increase in osmotic water flow. The reason for this lack of transepithelial water flow is unclear. We determined radiolabelled water flow across the filter supports using ^3H-H_2O. Our observation suggested that these commercial filters may be rate limiting for transepithelial water flow measurements (Candia et al., 1993).

Intracellular Ca^{2+} Concentration Measurements:

Cultured A6 and LLC-PK_1 cells were grown on coverslips (#0, Biophysica Technologies, Baltimore, MD) in 6-well plates (Costar). The medium was changed into new medium without serum and kept for 24 hours before Ca^{2+} measurement. On the day of the measurement, the cells were incubated for 60 min in HEPES buffered medium (NaCl 125 mM, KCl 5 mM, $CaCl_2$ 1.8 mM, $MgCl_2$, 2 mM, NaH_2PO_4 0.5 mM, $NaHCO_3$ 5 mM, HEPES 10 mM, glucose 10 mM, bovine serum albumin 0.1%, pH 7.2) containing 5 υM of a calcium fluorescent dye, Fura-2AM. The coverslip was then rinsed twice with the HEPES buffered medium.

The coverslip was mounted in a chamber on the stage of a Nikon Diaphot microscope. The chamber was filled with 3 ml of HEPES buffered medium and kept at 37°C during the experiment. Intracellular fluorescence intensity at 510 nm emission wavelength excited by alternating 340 and 380 nm excitation wavelengths was measured by a dynamic single cell video imaging method using with Image-1/FL Quantitative Fluorescence System (Universal Imaging Co., West Chester, PA). The intracellular Ca^{2+} concentration ($[Ca^{2+}]_i$) was calculated from the intensity ratio of

fluorescence at these two excitation wavelengths according to the equation of Grynkiewicz et al, 1985.

Three microliters of hormone and/or drugs were added into the chamber. The chamber was washed 3 times with HEPES buffered medium between additions of agonists.

RESULTS

SEM Morphometric Analysis:

Over twenty five comprehensive experiments were performed involving the whole toad urinary bladder tissues, cultured dissociated isolated single toad bladder cells and A6 amphibian kidney cortical cells, to analyze the results of exo- and endocytosis, and the role of PKC accompanying enhanced water flow process mediated by ADH and MZ. Previous morphometric and cytological studies associated with enhanced transmembrane osmotic water flow using the amphibian urinary bladder as a model have contained comprehensive description of the changes of the apical membrane surface and cytoplasm of the control unstimulated tissues along with tissues stimulated with ADH, calcium ionophore and other agents (Mia et al., 1983, 1987, 1988a, b). These studies contained little or no information on the effects of MZ, a non-phorbol activator of protein kinase C (PKC), on the morphocytological characteristics of the toad urinary bladder granular cells to define the role of PKC through ADH V_1 receptor interactions in the enhanced transmembrane osmotic water flow. Therefore, comprehensive time-dependent ultrastructural studies were carried out using unstimulated control, and ADH and MZ stimulated experimental bladder tissues under an osmotic gradient for 10, 30 and 60 min. Figures 3, 4 and 5 represent the

comparative surface substructural details (SEM) of the toad urinary bladder tissues following 10 min tissue treatment with ADH and MZ versus the control tissues. Figure 3 depicts the SEM surface view of such a control tissue as composed of predominant microridges, very similar to that reported in earlier studies (Mia et al., 1983, 1987, 1991a). Although the control tissues under osmotic gradient for 5 or 10 min retained predominant microridges network over the apical membrane surface (Fig. 3, arrows), few granular cells showed some degree of swelling and the appearance of some microvilli. Treatments with either ADH or MZ for the same time periods, altered the surface morphology with a dramatic appearance of a large number of microvilli over the plasma membranes of the granular cells as shown in Figures 4 and 5 (arrows) respectively. However, the size of microvilli at 10 min tissue treatment remained minute as they were barely elevated above the apical membrane surface. Tissues treated with a variable concentration of MZ ranging between MZ 10^{-6}M and 10^{-9}M for 5 min showed little difference in the number of granular cells with the propagation of microvilli and their size. However, longer tissue treatments for 30 or 60 min with either ADH or MZ caused a significant increase in the number and size of surface microvilli of granular cells as compared to unstimulated control tissues. Figures 6, 7 and 8 represent comparative SEM surface images of the control, ADH and MZ stimulated tissues respectively for 60 min, showing the relative microstructures of the apical membrane surfaces with predominant microvilli associated granular cells in ADH and MZ treated tissues than in the control tissues.

A morphometric analysis of the scanning electron micrographs (SEM pictures) of the control, ADH and MZ treated tissues for 10, 30 and 60 min was made to evaluate the relative increase in the number of granular cells with propagated microvilli. For this purpose, six scanning electron micrographs were taken from each tissue

treatment, each at a magnification of X3,000 representing 33 nm^2/area, for comparison. These results were statistically analyzed and plotted in histograms as in Figure 9. The histograms indicated a significant increase in the number of granular cells with microvilli in ADH and MZ treated tissues as compared to unstimulated control tissues during the corresponding time periods. The control tissues at 10 min (n=6) showed 13% of granular cells with microvilli in contrast to 53% in ADH (n=6) and 34% in MZ (n=6) treated granular cells respectively. The number of granular cells containing microvilli increased at 30 and 60 min tissue treatments showing 35% and 44% of control granular cells with microvilli as against 68% and 63% in ADH, and 74% and 64% in MZ treated tissues respectively. There appeared to be a steady time-dependent increase in the number of granular cells with microvilli, which seemed to level off at 30 min. The results of the ANOVA and Fisher's PLSD showed that there was no significant difference among the controls, whereas a significant difference at the 5% level was seen between the controls, and the ADH and MZ treated tissues. Figure 9 shows the percent of ADH and MZ induced microvillar granular cells against the control tissues. Concurrent water flow measurements indicated an enhanced transmembrane osmotic water flow across the toad urinary bladders associated with the actions of ADH and MZ compared to control tissues (data not shown).

A morphometric analysis was also carried out on A6 amphibian kidney cultured cells to evaluate the effects of ADH and MZ on the relative increase in the number of cells with surface changes vs. control tissues. Individual A6 cells, upon transfer onto ICN membrane supports or Anocell filter, undergo rapid growth to confluency to form a continuous polarized monolayer. Figure 10 represents a surface view of such monolayered control cells (vehicle treated, DMSO 0.002% for 60 min), grown on ICN filter supports. The apical membrane surfaces of these control cells, when viewed

under SEM, revealed the presence of a network of microridges along with distinct cellular tight junctions, similar to that seen with control toad urinary bladder tissues. When the A6 cells received stimulation by exogenous ADH or MZ for 60 min numerous microvilli from the continuous phase of the microridges were observed. The transformation of microridges into microvilli was also associated with some tissue swelling which resulted in the caving of the cellular junctions and the elevation of the apical membranes (Figs. 11,12). Treatment of A6 monolayer culture cells with ADH combined with MZ, also resulted in the formation of numerous microvilli and tissue swelling (Fig. 13). These results indicated that both ADH and MZ induced propagation of microvilli over the apical A6 cultured cells similar to those produced on the membrane surfaces of the toad urinary bladder tissues. This suggested that the remodeling of the apical membrane surface could involve activation of PKC.

Cytological Studies of Toad Urinary Bladders:

Ultrathin sections of the complementary control tissues as used in the SEM studies, when examined in the TEM, revealed a cytoplasmic profile with a composition of rough endoplasmic reticula, free ribosomes, mitochondria, golgi bodies and subapical secretory granules along the inner edge of the apical membrane (Fig.14, arrows). The apical membrane in control cell contained low elevations of microridges representing the TEM sectional views of the microridges seen in the SEM. Freeze fracture replica preparations with deep etching, with fracture line passing along the membrane surface horizontally, also revealed the portions of the microridges very comparable to the SEM images. In the TEM sectional views of the control tissues, the basolateral membranes between the adjacent granular cells (Fig. 15, short arrow) showed tight junctions and desmosomes with radiating tonofilaments and little or no

expression of membrane indentations. These control granular cells also contained an even distribution of dense cytoplasm and oval nuclei with dense heterochromatins occurring along the outer boundary of the nuclei (Fig. 14). The exposure of the control tissues to an osmotic gradient over a period of 30 min or longer caused a loss in the cytoplasmic and nuclear density (Fig. 15). However, the osmotic gradient did not cause any visible change in the secretory granules that normally reside beneath the mucosal membrane, which remained virtually intact (Fig.15, arrows).

Freeze fracture replica studies of the complementary control tissues also showed the distribution of the secretory granules beneath the apical membrane surface (Fig. 16, arrows) as seen in the TEM ultrathin sections. Although some control tissues showed apical microvilli over some granular cells, especially in tissues exposed to a prolonged osmotic gradient, they generally lacked cytosolic aggrephores or putative water channels when observed using freeze fracture preparations. This may explain the lack of apical membrane fusion events in control tissues and the decreased appearance of intramembrane particles (Fig.16). The effect of MZ on the cytoplasmic composition of the toad bladder tissues was rather dramatic, especially with tissues treated longer than 30 min. However, a 5 min tissue treatment with MZ also produced marked visible changes in the composition of the cytoplasm in some granular cells with an apparent increase in the distribution of microfilaments, microtubules (short arrows), fragmented rough-ER cisternae and swollen mitochondria with altered orientation of cristae (Fig. 17, long arrows). The effect of MZ may cause additional cellular disturbances involving the basolateral membranes which often appeared deeply indented in tissues that received exposure to MZ (Fig. 18, long arrow). The secretory granules that normally reside beneath the apical plasma membrane also showed a gradual loss in the granule contents following a brief MZ treatment (Fig. 18, short arrows). Tissues

which received treatment with MZ for 30 min or longer, showed a continuation of the process of degranulation of the cytosol and at 60 min, degranulation was complete showing virtually no sign of granules within the cytosol (Fig. 19). As seen in this TEM image mezerein treatment also caused significant tissue swelling, a loss in the density of cytoplasm and nuclei, and loosening of the intercellular junctions. Ultrathin sections from the ADH challenged complementary bladder tissues, when examined in the TEM, showed rough ER profiles with a variety of orientations from parallel to circular, a loss in the density of nuclei, as in MZ challenged tissues, but showed no discernible effects on the secretary granules as they appeared virtually intact in the subapical region (Figs. 20, 21, arrows). Parallel and circular profiles of the rough-ER cisternae in ADH stimulated tissues as seen in the TEM ultrathin sections may be revealed in the freeze fracture replica preparations as shown in Figure 22 (arrows). ADH treatment may cause enlargement off golgi cisternae and enhancement in their activities as golgi associated vesicles increased and enlarged (Fig. 23) as compared to control tissues (Fig. 24). This finding suggests that golgi bodies stimulated by ADH, could induce active synthesis of associated vesicles at the trans-golgi regions. Such images of golgi complexes with insipid activity in the control and amplified activities in the ADH treated tissues were often encountered in TEM sections.

The presence of water channels (aggrephores) in the cytosol and the occurrences of the apical membrane fusion events were investigated on control, ADH and MZ challenged tissues using the techniques of freeze fracture. In freeze fracture replicas, aggrephores are generally recognized as somewhat conical membrane structures studded with minute protein particles. Most commonly the aggrephores were reported to be present in the subapical region of the cytoplasm with an angular orientation toward the apical membrane for possible insertion following tissue stimulation with

ADH (Mia et al., 1991b). Whereas the fusion events at the membrane surface often appear as clusters of particles with a stellar distribution. A description of the particles and membrane fusion in toad urinary bladder tissues is provided in the schematic illustration in Figure 1. In freeze fracture replicas, the control unstimulated tissues showed an apparent lack in the distribution of either the aggrephores or the number of apical membrane fusion events, even though the tissues were retained under an imposed osmotic gradient for 60 min. However, the toad bladder tissues which were challenged with ADH or MZ for 60 min, showed the presence of aggrephores or putative water channels and increased fusion events (Figs. 25, 26, arrows). Actual counts of the membrane fusion events made from a number of freeze fracture replicas indicated that their incidental distribution in the stimulated bladder tissues to be in the order of $2/nm^2$ area in the ADH (Fig. 25) and $2/nm^2$ area in the MZ treated (Fig. 26) tissues, while in control tissues it was $< 1/nm^2$.

Bladder sacs that received treatment with verapamil, an inhibitor of ADH stimulated water flow across the amphibian urinary bladder, caused not only an accumulation of numerous secretory granules in the granular cells (Mia et al., 1991a, b) but also a concomitant depression in the incidence of cytoplasmic aggrephores and membrane fusion events, and therefore, a sparse distribution of intramembrane particles. If ADH is added to the incubating media in the presence of verapamil, transmembrane water flow response was somewhat restored as well as the incidence of aggrephores and membrane fusion events (Fig. 27, arrow), indicating the ability of ADH to reverse the actions of verapamil, possibly through increasing intracellular calcium.

Role of PKC in Transmembrane Water Transport:

In order to evaluate the role of PKC in the actions of vasopressin, we conducted a series of experiments to track PKC activation and translocation using immunofluorescent and immunohistochemistry techniques. PKC translocation can be observed using selective antibodies for PKC isoforms, immunofluorescent labeling and FITC (Simboli-Campbell et al., 1993). Since little is known about the actions of PKC on vasopressin-mediated water transport process nor its distribution in renal epithelia, we carried out immunogold antibody detection labeling of PKC subtypes I, II and III using specific monoclonal antibodies and protein A or G-gold probes. Indeed, immunogold labeling studies showed that gold particles were distributed singularly and in discrete isolated clusters in the cytosol as well as in the apical membrane domains essentially in tissues which received stimulation with either ADH or MZ. Figures 28, 29 and 30 are TEM images demonstrating the presence of PKC isozymes subtypes I, II and III in MZ (Figs. 28, 29, arrows) and ADH (Fig. 30, arrow) stimulated tissues respectively. These isozymes are distributed singly and in clusters within the cytosol with a concentration of gold particles over the diffused cytoplasmic bodies. The physical appearance of the cytosolic diffused bodies and the distributional patterns of gold particles, regardless of their isoforms, remain remarkably similar in both tissues that received stimulation with MZ and ADH. At times, clusters of gold particles in diffused cytoplasmic bodies (Fig. 31, short arrow) were found among a large number of microfilaments (Fig. 31, long arrows) suggesting a possible association of PKC with microfilaments. This association could be important to the translocation process of PKC to the apical membrane. Gold particles appearing in association and/or within the microvilli (Figs. 32, 33, 34, arrows) also suggested possible migration of PKC from the cytosol into the microvilli and perhaps, along with the putative water channels

for apical membrane fusion. Double immunogold labeling, achieved by exposing single grids sequentially to PKC subtypes II and I with intervening exposures to protein A-gold (5 and 20 nm) probes respectively, showed that these PKC subtypes localized separately in discrete bodies or co-localized in the same cytoplasmic body as well as in the apical membrane sites (Fig. 35, arrow) in tissue treated with either MZ or ADH. Expression of protein A-gold particles over the dense bodies in the cytoplasm and on the apical membrane domains indicated possible translocation of PKC enzymes to the apical membrane in a time course that was similar to the insertion of cytoplasmic water channels into the apical membrane following hormone addition (Mia et al., 1991b). Control tissues exposed only to 0.1% BSA and protein A-gold or protein G-gold particles failed to show any appreciable labeling (Fig. 36). Expression of protein G-gold involving isozyme III (α) was seen to be localized in isolated patches rather than in discrete diffused bodies as seen with protein A-gold probes (Mia et al., 1991b).

Immunofluorescent localization of PKC subtype III was also performed using a specific monoclonal antibody against this PKC isoform and fluorescein isothiocyanate (FITC) IgG, to reveal the global distributional pattern of this isozyme subtype in cultured renal tubular cells, A6 amphibian kidney cells. The A6 cells, grown on glass cover slips quickly formed confluent monolayers and cellular tight junctions as seen under SEM (Figs. 10-13). Phase contrast micrographs of the confluent monolayer on glass cover slips demonstrated that these cells form a continuous monolayer sheet (Fig. 37) and were found suitable for immunofluorescent microscopy. These studies revealed the localization of PKC isozyme III in the cytoplasm and also possibly associated with membranes in particulate forms in the ADH and MZ stimulated cells (Figs. 38, 39), very similar to the diffused bodies discovered in the toad urinary bladder tissues following immunogold antibody labeling of the tissues. Control tissues only exposed

to 0.1% BSA showed little or no presence of fluorescence (Fig. 40).

Analysis of the Distribution of Gold Particles Associated with PKC Isozymes:

Quantitation of the distribution of the gold particles associated with PKC isozymes I, II and III were made from the control as well as from the ADH and MZ challenged toad urinary bladder tissues. The gold particle counts were made from electron micrographs, involving the control grids BSA (n=26), anti-PKC I (n=10), anti-PKC II (n=10), anti-PKC III (n=7), PKC III+anti-PKC III (n=5), ADH grids BSA (n=44), anti-PKC I (n=26), anti-PKC II (n=11), anti-PKC III (n=10), and MZ grids BSA (n=9), anti-PKC I (n=32), anti-PKC II (n=10) and anti-PKC III (n=12). Each electron micrograph was taken at X30,000 magnification within an area of 33 nm^2/picture, and at random with greater particle density. Statistical analysis, performed on data from gold particle counts were expressed in individual histograms for each PKC isoform to evaluate the relative distribution of gold particles. The distribution of gold particles, calculated for each PKC isoform, was found to be significantly higher in tissues exposed to ADH and MZ compared to the BSA exposed control tissues. The histogram in Figure 41 represents the summation of the total gold particle counts for all three isozymes involving the control (n=111), ADH (n=47) and MZ (n=54) stimulated tissues. The distribution of gold particles in ADH and MZ treated tissues was significantly higher as compared to the control tissues. Blocking the antigenic sites in the control tissue sections with a mixture of PKC isozyme III and anti-PKC isozyme III prior to exposure to protein A-gold probes resulted in no appreciable labeling of this PKC isozyme with gold particles beyond that observed for the other control tissue sections.

Identification of PKC Isozymes Using Western Blot Analysis:

In addition to immunogold and immunocytochemical approaches to identify the various PKC isozymes, we developed procedures to separate cellular proteins from both the cytosolic and membrane fractions of toad urinary bladder dissociated granular cells using SDS-PAGE electrophoresis and a BIORAD mini gel system. In these studies, we used 10% dissolving and 5% stacking gels for electrophoresis. Following electrophoresis, the samples were blotted to nitrocellulose filter paper which was blocked by immersion in "Blocking Buffer" (3% skim milk in PBS) for 2 hrs at 8°C. The nitrocellulose was washed and incubated with the primary antibody solution for 2-3 hrs at room temperature. The filter was then washed several times and incubated in the "secondary antibody solution" for 1 hr at room temperature. Following incubation the filter was washed in PBS-0.05% Tween 20 for 3-5 min with constant rocking. The filter was then washed and developed in freshly prepared alkaline phosphatase substrate solution. Figures 42 and 43 represent photographs of the SDS-PAGE gel of proteins isolated from the dissociated toad urinary bladder cells, and a western blot of this gel respectively showing the presence of PKCα (Fig. 43, arrows) on both the membrane and cytosolic fractions of the toad urinary bladder epithelial granular cells. Upon stimulation by ADH, there was an increase in PKC-associated enzyme on the membrane fraction suggesting the hormone enhanced translocation.

Influence of Filter Supports On Transport Characteristics of Cultured A6 Kidney Cells:

One of the aims of this project was to develop an *in vitro* model that can be used to assess the water transport processes regulated by vasopressin. Cultured renal epithelial cells could provide an alternative "membrane model" system to study

antidiuretic hormone (ADH) action and transepithelial water transport. Renal epithelial cells of native epithelia, like kidney and toad urinary bladder epithelia, rest on their natural support. These supports represent a low restriction to the transepithelial movements of ions and fluid. Therefore, movement of ions and water across a preparation consisting of the epithelium with its connective tissue is mainly dictated by the permeability properties of the epithelial layers. We have developed an *in vitro* tissue culture model of amphibian kidney cortical cells (A6 cells), grown on various filter supports. Although epithelia grown on permeable filter supports develop polarization and tight junctions as indicated by their electrical properties and morphology, the rate of transport of ions in these tissues is usually lower than in the native tissue. This deficiency was justified as due to the artificial conditions of the tissue culture environment in which A6 cells were grown. Despite the large number of electrophysiological studies using A6 cells, few have measured unidirectional Na or Cl fluxes across the filter supports alone without cell monolayer (Candia et al., 1993). A most puzzling finding was the lack of net water flow under an osmotic gradient when cultured cells on filters were stimulated with ADH on Anocell (Fig. 44) or Cellagen (Fig. 45). This negative water flow response was not due to a lack of functioning receptors, as we could demonstrate an increase in the formation of cAMP in these cells grown on filter supports (Fig. 46). In addition, these cells grown on either Anocell filters or Cellagen filters, responded to ADH with changes in cellular surface morphology as shown in our SEM (Figs. 10-13) studies, very similar to that seen in the intact tissues. Although bulk flow elicited by an osmotic gradient (J_v) did not change following addition of ADH, changes in diffusional flow (J_{dw}) could take place and be measured. Therefore, unidirectional tritiated water fluxes (THO) were determined in A6 cells grown on Anocell filter supports. The results indicated no change in

unidirectional THO fluxes with either 50 or 200 mU/ml of ADH (Fig. 47). The observed fluxes corresponded to a constant value of J_{dw} of about 1.3 x 10^{-4} cm/sec. This observation, coupled to the findings of no osmotic water flow response to ADH, suggested that A6 cells were lacking some critical component essential for the ADH transepithelial water flow response. However, because we were observing a constant value for J_{dw}, we decided to adjust the rate of water flow across the limiting barrier at the apical surface by the addition of amphotericin B, a polyene antifungal agent or by administering digitonin, a solubilizer. Neither of these agents, when added to the apical surface, were able to enhance unidirectional THO fluxes (Fig. 48). Yet, amphotericin B in the same cells increased ion transport while decreasing transepithelial resistance. These results suggested that there was an unknown barrier in series with the apical membrane limiting water flow. To test if the filter itself represented a barrier for water diffusion, THO fluxes were measured across Anocell filters without an associated cell culture monolayer. As seen in Figure 49, the THO fluxes of freshly mounted filters decreased with increasing time and reached equilibrium at approximately 3 to 4 hrs. The decrease in THO flux correlated to a measured increase in filter resistance, which also increased with time (Fig. 50). J_{dw} decreased from an initial value of about 35 to a stable value of 7 ul/min cm^2. More remarkable was the fact that in most individual filter preparations, control values of J_{dw} were very stable and changed little under hormone stimulation or other experimental manipulations. These results suggested that the filters were rate limiting to water flow (Candia et al., 1993). Anocell filter supports seem to be hydrophilic. Fluid placed on its cupped inner surface does not wet its outside surface even after several hrs. Other filters tested also appeared to have a limited capacity to pass fluid. Our findings suggested possible limitations of filter supports for cultured studies, particularly those involving water flow studies using the

extracellular matrix on which epithelia perform their physiological functions.

ADH V_1 Versus V_2 Interactions

Our laboratory showed that MZ mimicked vasopressin in mediating an osmotic water response, suggesting that activation of PKC could play a role in regulating transepithelial water flow. Recently, Teitelbaum and Straheim (1990) demonstrated that rat inner medullary collecting tubule cells contained a vasopressin V_1 receptor coupled to an increase in phosphinositide hydrolysis, and this response occurred at low hormone concentrations below that needed to increase adenylcyclase. Our laboratory investigated the relationship between the cAMP effects of vasopressin and its effects on calcium mobilization using the A6 amphibian kidney cell line. These cells, derived from the cortical collecting tubule of the amphibian *Xenopus laevis*, when grown on filter supports showed the electrical properties of transepithelial potential difference (PD), short circuit current (Isc) and resistance (R) as measured by mounting the filter support in a Lucite chamber (Candia et al., 1993) similar to that seen in other renal epithelia. Under basal conditions the confluent A6 monolayer of amphibian kidney cultured cells showed a PD of 37 mV and a resistance of almost 5 kohms (Fig. 51). Following the addition of vasopressin, a decrease in resistance and an increase in the Isc was seen. The increase in Isc appeared to be mediated through an increase in sodium transport as amiloride, a sodium channel blocker, inhibited the hormonal increase in transport. These results demonstrated that these cultured cells were responsive to vasopressin, and that they contained an active V_2 receptor coupled to adenylcyclase activity. To support this observation we measured cAMP formation in these cells using adenine labeling method. Vasopressin produced a dose-dependent (Fig. 52) and time-dependent (Fig. 53) increase in cAMP formation indicating the

presence of a functional adenylcyclase enzyme coupled to V_2 receptors (Fig. 53). We also investigated the interaction between PKC and activation of adenylcyclase to determine if the V_1 receptor negatively regulated the V_2 response. The PKC activation with MZ had no effect on the ability of vasopressin to stimulate cAMP formation (data not shown).

Calcium Signalling and the Actions of ADH:

Previous studies in our laboratory suggested that the effects of ADH on the activation of protein kinase C appeared to involve vasopressin V_1 receptor activation. It has been suggested that the release of intracellular calcium may serve as a second messenger to activate enzymes essential in the regulation of transepithelial water transport. We utilized video image analysis to ascertain the effects of vasopressin on intracellular free calcium concentrations. In particular, we attempted to determine which of the ADH receptors were responsible for the increase in calcium concentrations mediated by AVP. In this study the fluorescent dye, Fura-2AM, was used to measure free intracellular calcium in LLC-PK_1, cultured kidney cells. We selected the porcine cell line to investigate this effect, as the mammalian cortical kidney had been shown to contain V_1 receptors. Figure 54 represents the SEM surface view of the unstimulated control LLC-PK_1 porcine kidney cultured cells grown on Anocell filter supports. It can be seen that these cells possess a distribution of scattered microridges with no clearly defined cellular identity off the individual cells as seen from the surface. In order to monitor calcium changes, the cells are loaded with the Fura-2AM. This dye permeates the cell in its ester form. Once in the cell esterases convert the dye to Fura-2 which is free to interact with calcium, where the dye fluorescence is proportional to the calcium concentration in the cell. A ratio fluorescence technique,

using a dual excitation computer controlled video image system allows monitoring of intracellular free calcium in real time.

As can be seen in Figure 55, 10^{-8} M AVP increased intracellular calcium in LLC-PK_1 procine kidney cultured cells. These cells, derived from the porcine kidney distal convoluted tubule, are known to be the site of vasopressin actions. Figures 56 and 57 compare the response of AVP to oxytocin, another peptide that has known antidiuretic effects in some kidney models. Oxytocin which also contracts smooth muscles by increasing intracellular calcium, acts on receptors which appear to be oxytocin receptors, since the increase in calcium by oxytocin appeared to be blocked by an oxytocin peptide antagonist (Fig. 58). Surprisingly, the effects of AVP on intracellular calcium were blocked by the oxytocin antagonist (Fig. 59). This is demonstrated quite readily in Figure 60, where AVP effects before and after the oxytocin antagonist are presented. The antagonist completely abolished the actions of AVP on calcium mobilization. Additional experiments are planned to test the actions of AVP and oxytocin in the presence of a vasopressin antagonist (V_1), to determine if the receptor in the porcine kidney cells does not differentiate between these two peptides, oxytocin and vasopressin. Therefore we are still uncertain of the receptor that is coupled to the calcium signalling process in the kidney, and further experimentation is warranted.

Retrieval of Water Channels by Endocytosis:

Our studies indicated that an increase in intracellular calcium by PKC activation may play an important role in the insertion of water channels following hormone activation. What was unclear were the processes that regulate water channel retrieval following removal of hormone or following desensitization or down regulation.

The technique of scanning electron microscopy was used to evaluate the surface substructure changes that occur following removal of hormone and mezerein subsequent to tissue stimulation with ADH and MZ. The main purpose of this series of experimental studies was to understand the mechanism and regulation of membrane internalization following withdrawal of ADH and MZ. This process often labelled endocytosis, occurs as a means of maximizing water channel recycling. This experiment also served to evaluate the role of protein kinase C in apical membrane retrieval during endocytosis.

Apical membrane internalization was induced by stimulating the bladder tissues with ADH or MZ for specified times and removing the hormone and/or drug to allow for retrieval. Control, ADH and MZ challenged tissues, following incubation for 10 or 15 min, received two quick fresh buffer rinses to remove the ADH or MZ. These tissues were then allowed to recover separately for 5, 10, 15, 20, 30 and 60 min. The SEM analysis of the apical surface topography revealed that the control tissues, regardless of the length of time under an osmotic gradient, showed little or no sign of apical membrane internalization in the form of inpocketting of the apical membrane during the retrieval period. Many scanning electron micrographs of control tissues, representing each stage of 5, 10, 15, 20, 30 and 60 min retrieval periods, were studied and found to show a general lack of apical membrane surface changes indicative of endocytosis. Figures 61 and 62 are representative SEM images of the apical membrane microstructure environment of such a control tissue showing the apical membrane as composed of a continuous distribution of microridges. In contrast, comparable tissues, following removal of ADH or MZ resulted in apical membrane invaginations coincident with the retrieval of water channels by endocytosis. The molecular and cellular mechanisms that may interplay to induce this apical membrane remodeling are

unknown. Figures 63 and 64 depict the surface configuration, as displayed by ADH and MZ stimulated tissues, during a 5 min retrieval period. A number of granular cells developed prominent invaginations over the mucosal surface area (Figs. 63, 64, arrows). The percent of the granular cells showing the loss of surface villi as an index of endocytosis was 3% in the control as opposed to 31% and 4% in the ADH and MZ stimulated toad urinary bladder tissues respectively involving 5 min retrieval time period (Fig. 65).

The apical membrane retrieval process in toad bladder tissues, as triggered by removal of ADH or MZ, appeared to be progressive. Therefore, various stages of endocytosis during time periods post hormonal or drug washout were studied. The retrieval process began with several slight surface invaginations each of which exhibited elevated margins (Figs. 66, 67, arrows). These invaginations, in most cells, were found to coalesce laterally to form a single large invagination across the entire membrane surface of the granular cells. Ultrathin sections also revealed the presence of surface invaginations (Fig. 68), analogous to that seen in SEM images (Fig. 67). At 10, 15 or 20 min following withdrawal of ADH or MZ, the toad urinary bladder surfaces were seen to have a large number of endocytotic pits (Figs. 69, 70, arrows). Endocytosed pits were smaller in number in tissues exposed to MZ as compared to those seen in ADH treated tissues. Cell counts at 10 min retrieval, indicated that fewer than 8% of the cells showed surface invaginations and putative endocytosis in MZ exposed tissues (n=6), as compared to 45% of the cells in ADH stimulated tissues (n=6) (Fig. 65). The incidence of proposed endocytosis in MZ and ADH treated tissues differs with time of retrieval. Therefore, at 20 min retrieval, 35% of the MZ cells showed endocytosis compared to 17% of the ADH treated cells (Fig. 65). These tissues when examined in the TEM using the ultrathin sections, revealed pits as large

vacuoles (Fig. 71, arrows) essentially localized beneath the apical membranes and not associated with the basolateral or basal plasma membrane. In some sections, coated vesicles originating from the apical as well as from the basal membrane, were seen scattered within the cytosol of ADH stimulated tissue (Fig. 72, arrows). Freeze fracture and deep etching preparation of bladder tissues stimulated with ADH also revealed the presence of coated vesicles attached to the membrane (Fig. 73, arrows) very similar to coated vesicles seen in the ultrathin sections in the TEM. Presence of large endocytosed vacuoles within the cytosol resulted in the displacement of the nuclei against the basal membrane. As a result, the nuclei surrounded by vacuoles may assume a variety of shapes (Fig. 71).

Control tissues, under an imposed osmotic gradient for 15 min, had an average fluid loss from the bladder sac of 2 μl/min (n=4), whereas ADH challenged tissues had 41 μl/min fluid loss (n=4). Apical membrane surface changes in ADH stimulated tissues reached a peak at 10 or 15 min into the retrieval period, with a percent of cells involved at 46% and 64%, respectively. Whereas in the control tissues, less than 5% of the cells were involved (Fig. 65). During the process of the formation of invaginations, apical membrane surfaces tend to undergo membrane remodeling with a loss of both microvilli and microridges in both ADH and MZ stimulated tissues (Figs. 67, 70, arrows) leaving flattened membrane surfaces with no visible microstructure. In ultrathin sections, such membranes appear to contain no microridges or microvilli. This phase of membrane disposition may represent a membrane transition during transformation of microvilli into microridges. These tissues when challenged with MZ, 10^{-6} M for 15 min, and later exposed to PKC I antibody and protein A-gold particles using ultrathin sections, showed localization of gold particles in association with anti-PKC I, predominantly surrounding the coated vesicles as shown in Figures 74 and 75 (arrows). It is not

known whether the coated vesicle originated from the apical membrane, or migrated into the cytosol during the apical membrane restoration process. However, the evidence indicates that this may occur as the presence of several of these coated vesicles, laced with gold particles, appear to have migrated from the apical membrane into the cytosol (Figure 76, arrows). This may suggest a possible link between the incidence of coated vesicles and the endocytic process for membrane restoration. These coated vesiclecs appeared to be associated with membrane cisternae surrounding a central cavity. Coated vesicles were encountered in TEM ultrathin sections and freeze fracture preparations (Figures 72 and 73). Also these coated vesicles are distinctly different than the caveolae which are released from the membrane surfaces of the microfilament-rich cells present in toad urinary bladder sacs (Fig. 77) and also reported by Smart et al., (1994) to occur in other cell types.

The studies of membrane restoration by endocytosis as affected by ADH or MZ were extended to include 30 and 60 min periods following removal of hormone or drug. In addition, water flow rates were measured from bladders with or without adjusting the osmotic gradient during the 60 min retrieval period, following withdrawal of ADH. The recovery of the water channels from the apical membrane in ADH or MZ exposed tissues begins soon after the removal of the ADH or MZ. However, such membrane remodeling processes were seen to be gradual, as not all the granular cells had undergone a restoration of the apical membrane even after 30, or 60 min into the retrieval periods following withdrawal of ADH or MZ. Global surface views of apical membranes at 30 and 60 min following ADH (Fig. 78) and MZ removal (Figs. 79, 80) showed that, although a large proportion of the granular cells had restored surface morphology as in the pre-hormone normal state, a few granular cells still had some surface microvilli, while other membrane components

showed the presence of surface remodeling. Closer views are presented in Figures 81, 82 and 83 to demonstrate the membrane restoration in the granular cells showing almost complete reorganizational pattern of the microridges surrounding the endocytosed pits.

The question remained, however, was this surface remodeling consistent with changes in transepithelial water flow and was the retrieval of water channels a consequence of osmotic gradient changes? Furthermore, will maintaining the osmotic gradient sustain the water flow response and support water channel maintenance at the apical membrane? Experiments were therefore designed to test the hypothesis that continued water permeability was dependent, in part, on the osmotic gradient for water flow. Bladders were set as sacs and ADH was added after an initial baseline water flow measurement. ADH was then removed from both the bladder sacs, and the sacs were then allowed to retrieve. During this retrieval period, the osmotic gradient was maintained in one sac by replacing the fluid inside the bladder sac with fresh diluted Ringer's solution, while the other sac was left with no periodic buffer rinses. These results indicated that maintaining the osmotic gradient did not restore or maintain the rate of higher flow, rather water flow was found to return to baseline faster if the gradient was not allowed to dissipate (Fig. 84). SEM studies also indicated that there was little or no difference in membrane restoration in tissues which received periodic adjustments of the osmotic gradient.

To quantify the extent of endocytosis during retrieval, counts of the endocytosed pits were made at 20, 30 and 60 min into the retrieval periods (Figure 64). It was seen that during the 20 min retrieval period, the number of individual cells showing endocytosis in MZ stimulated tissues was 35% as compared to 17% in ADH stimulated tissues. During 30 and 60 min retrieval periods, the number of the involved cells in

ADH stimulated tissues was found to be 27% and 23% versus 22% and 9% in MZ stimulated tissues respectively, whereas fewer than 2% of the control cells showed signs of endocytosis. The results indicated that MZ stimulated tissues responded to endocytosis slower than ADH stimulated tissues, and corresponded with slower water loss from the MZ challenged tissues.

DISCUSSION AND CONCLUSIONS

Biological membranes are dynamic cellular structures that are not only responsible for limiting the permeability of the cell, but also play a role in the regulation of a variety of cell functions. Eukaryotic cells, such as those of granular cells in renal epithelia and toad urinary bladder, through the process of specialization, have acquired complex, yet integrated molecular and cellular processes to recycle plasma membrane components and proteins as a means to regulate a variety of crucial cellular functions. Internal membrane shuttling is an important process for renal cortical cells as a means to regulate osmotic water flow, particularly, at times where water reabsorption was essential to prevent dehydration. The process of transepithelial water flow in renal tissue includes two important biological events involving exocytosis and endocytosis for cycling of water channels in vasopressin responsive tissues. A schematic presentation of exo- and endocytosis involving ADH V_2 and V_1 receptor interactions is shown in Figure 1. The second messenger pathways in the normal unstimulated cells, and hormone-stimulated toad urinary bladder cells is presented, as well as following removal of hormone. The exocytic process occurs as a consequence of ADH actions on its receptors and is initiated for selectively packaging water channels (aggrephores) for export to the apical membrane for fusion (Kachadorian et al., 1977; Wade et al.,1981; Davis et al., 1982; Hays, 1983). Whereas the process of endocytosis

following removal or suppression of hormone actions occurs in order to recover portions of the apical membrane, water channels, likely as coated vesicles, would also be returned to the cytoplasm (Pearse and Crowther, 1987; Brodsky, 1988; Schmid, 1992). Little is known about the fate of these water channels in toad urinary bladders, once they are internalized into the cytosol. Therefore, a major challenge in transmembrane fluid transport dynamics is to determine the molecular and cellular mechanisms of exo- and endocytosis of water channels and the processes of regulation for maximizing the reabsorptive capacity of the kidney. Our laboratory has been concerned with identifying the key components involved in these dynamic cellular processes, and have conducted a series of experimental studies using the toad urinary bladders as a renal model to determine both structurally and biochemically the characteristics of water reabsorption by vasopressin..

Vasopressin stimulation causes rapid transmembrane osmotic water flow in renal epithelia as well as in the toad urinary bladder by a process that involves exocytosis of water channels. The enhanced water flow is believed to occur through stimulation of ADH V_2 receptors coupled to adenylate cyclase, enhanced cAMP formation and activation of protein kinase A (Handler and Orloff, 1973; Schlondorff and Levine, 1985). These biochemical events are necessary precursors to the insertion of water channels (aggrephores) into the apical plasma membrane (Chevalier et al., 1974; Kachadorian et al., 1978; Hays et al., 1985). The insertion of water channels is thought to involve the cytoskeletal system of microfilaments and microtubules (Hays et al., 1985; Taylor et al., 1973; Hardy and DiBona, 1982; Pearl and Taylor, 1983; Mia et al., 1991a). The apical membrane fusion of water channels results in an increase in membrane capacitance following stimulation with vasopressin. This occurs in renal epithelia, as well as the amphibian urinary bladder resulting in enhanced osmotic water

flow.

The importance of microfilaments in the intracellular transport process has been the subject of a recent article (Stossel, 1994), and we anticipate additional studies of the role of microfilaments and microtubules in understanding the mechanism of the cycling of water channels in transepithelia water transport.

In the normal unstimulated control tissues, the apical plasma membrane, regardless of tissue types, contains a smooth surface configuration with a continuous phase of microridges. Intact toad urinary hemibladders as well as the isolated dissociated toad bladders granular cells, retained in the Ringer's solution for controls, showed a remarkable similarity with that of the cultured amphibian A6 kidney cells, and LLC-PK1 porcine kidney cells grown on either Anocell or ICM membrane filters (Candia et el.,1993). Once these cells are exposed to either ADH or MZ or to a combination of ADH and MZ, they showed membrane conformational changes representative of a conversion of the apical microridges into numerous prominent microvilli which were associated with tissue swelling. In the normal unstimulated control tissues, the apical membrane of toad urinary bladder granular cells contain essentially a smooth surface with a continuous phase of microridges. However, many of the control granular cells were also found to have microvilli over the apical membrane surfaces, and the villi formation was seen to be progressive with prolonged tissue treatment under osmotic gradient. The reason for such transformation of microridges into microvilli in control tissues is unknown. It could be due to the presence of osmosensitive cellular compartments or a result of the osmotic difference, hypertonicity or stretch, or a combination of these factors could stimulate villi formation in amphibian bladder epithelia (Mills and Malick, 1978; Dratwa et al., 1979; LeFurgey and Tisher, 1981).

We also demonstrated that MZ, a non-phorbol activator of protein kinase C (PKC), increased transepithelial water flow when added to the mucosal surface of toad urinary bladder sacs (Yorio and Satumtira, 1989) mimicking the actions of ADH. However, when bladders were exposed to MZ for 30-60 min and then challenged with ADH, the hormone effect on water flow was attenuated at 30 min and completely blocked following 60 min preincubation with MZ. These results suggested that MZ, via PKC activation was acting on a pathway similar to that stimulated by hormone. Since long incubations (as with 60 min) with PKC activators, like MZ, are known to down regulate PKC activity, PKC activity may be important for water flow to occur. Additional studies suggested that activation of PKC by MZ caused premature insertion of water channels into the apical membrane prior to the actions of hormone on V_2 receptors and activation of protein kinase A. It was found that the enhanced water flow induced by MZ, similar to ADH action, correlated with the conversion of the apical microridges into numerous microvilli. Similarly, water flow, as enhanced by MZ, was further found to be correlated with an increased incidence of cytosolic aggrephores (water channels) and concurrent events of apical membrane fusion in freeze fracture preparations (Mia et al., 1989b) similar to that found with ADH stimulated tissues (Chevalier et al., 1974; Hays et al., 1982, 1985). This suggested that PKC may have a functional role in the regulation of the insertion of water channels during enhanced transmembrane water flow.

Protein Kinase C, a calcium and phospholipid-dependent protein kinase, exists in various isoforms in a variety of tissues and is known to play a key role in the regulation of a variety of intracellular processes, including signal transduction (Yoshida et al., 1988). In our studies, we demonstrated the presence of PKC isozymes in toad urinary bladder following stimulation with ADH and MZ to indicate that the amphibian

urinary bladders also contained a hormone-activated PKC pathway probably through stimulation by vasopressin of V_1 receptors. The stimulation of this receptor results in the breakdown of polyphosphoinositides and the formation of inositol trisphosphate and diacylglycerol (Yorio et al., 1985; Yorio and Satumtira, 1989).

In support of the role of the ADH V_1 receptor and activation of protein kinase C in the augmentation of osmotic water flow, we have shown that mezerein, a non-phorbol activator of protein kinase C can enhance osmotic water flow, as well as cause apical membrane transformations and remodeling similar to that produced by challenges with ADH (Mia et al., 1983, 1987). Further evidence in support of the role of PKC was derived from several experiments in which three protein kinase C isoforms were localized at the fine structural level using PKC antibodies and immunogold antibody labeling techniques in toad urinary bladder tissues. The gold particles occurred singular or in association with cytoplasmic dense bodies following stimulation with hormone or PKC activation by MZ. Immunogold particles also appeared in the apical membrane domain following hormone MZ treatment demonstrating PKC translocation. The control tissues seldom showed localization of any of the PKC isoforms in the cytosol or in the apical membrane domain. Failure to label the protein kinase C isoforms in control tissues of toad urinary bladders by protein A-gold probes may likely be due to their presence in soluble forms in the control tissues and/or in a structural form not necessarily recognized by the antibodies and the protein A-gold probes. In addition, these dense bodies, occurring among the mitochondria, nuclei, rough-ER etc., were the only cytoplasmic structures found to be predominantly laced with gold particles, while leaving other organelles free of gold particles. The presence of gold particles was not found to be associated with any other organelles, including the nuclei as was reported for NIH 3T3 cells (Leach et al., 1989). The detection of PKC subtypes alone in the

granular cells in toad urinary bladder tissues suggest that PKC may be a key player in regulating ADH mediated water flow, concurrent with water channel translocation following stimulation with hormone. Additionally, the identification of PKC isoforms on dense granules prior to translocation may suggest a pathway for enzyme movement from cytosol to membrane on discrete PKC carrier proteins or associated water channels.

The physical appearance and the distribution patterns of PKC isoforms are very similar to one another, and there appeared to be no apparent difference between the diffused bodies labeled with gold particles in tissues stimulated with MZ or ADH. The gold particles were found to be distributed singularly and concentrated in diffused cytoplasmic bodies or in association with the apical plasma membrane. The diffused cytoplasmic bodies involving the three PKC isozymes, as labeled with gold particles, were found only in the granular cells of the toad urinary bladder and not in any other cells, including the mitochondria-rich, microfilament-rich and goblet cells. Immunofluorescent studies using PKC antibodies and fluorescein isothiocyanate (FITC) carried out by other workers indicated that some PKC isoforms occurred in the cytosol and in the nuclei in particulate forms following stimulation with phorbol esters (Jaken et al., 1989) and in the unstimulated cultured MDBK renal epithelia (Simboli-Canpbell et al., 1993). We also demonstrated the presence of several PKC subtypes in toad urinary bladder granular cells and in A6 amphibian kidney cultured cells following stimulation with ADH and MZ, using PKC antibodies and protein A-gold probes at the fine structural level, and fluorescein isothiocyanate (FITC) at the light microscopy level, indicating a functional role of PKC in hormone stimulated tissues.

Several observations prompted our attention to undertake experimental studies on the phenomenon of membrane retrieval and membrane remodeling following

hormone removal. The cellular events leading to the process of endocytosis have been recently investigated and the biochemical characterization of clathrin coated pits associated with endocytosis in a variety of tissues has also been described (Brown, 1989; Pearse and Crowther, 1987; Schmid, 1992). However, little is known about the structural and morphological changes that accompany the process of endocytosis. Using the techniques of SEM, we examined the surface membrane remodeling of the toad urinary bladder granular cells that may be associated with the endocytotic retrieval of membrane components, i.e., water channels, following removal of vasopressin (Brown, 1989, Brown et al., 1990, Coleman et al., 1987). In addition, it was not known if PKC was involved in the retrieval process during endocytosis. The current observations suggest that the apical plasma membrane surface of toad urinary bladders, passes through stages of membrane remodeling that is coincident with the retrieval of water channels prior to the restoration of the membrane to its normal surface topography containing microridges. In addition, the processes of exo- and endocytosis, with reference to surface fine structure, were not previously evaluated in time-course studies using a single tissue system responsive to vasopressin. This is particularly relevant to the regulation of these two processes involved in the overall intracellular cycling of water channels in ADH responsive tissues. Hence, the current research reports on both the processes of exo- and endocytosis using a variety of renal epithelia as ADH responsive model membranes.

The plasma membrane cycling of ADH stimulated water channels in amphibian urinary bladder tissues, as well as in the renal cortical cells are accomplished by cellular events involving exo- and endocyotsis. The process of exocytosis has received adequate attention and appears to involve the export of proteinaceous water channels or aggrephores, normally found in the cytosol of the unstimulated bladder tissues, to the

apical plasma membrane for incorporation as a means to enhance water flow (Humbert et al., 1977; Muller and Kachadorian, 1984; Wade, 1978). Enhanced apical membrane water permeability by ADH is correlated with a restructuring of the apical membrane microridges into numerous microvilli with an increase in membrane surface area and capacitance (DiBona et al., 1969; DiBona, 1981; Spinelli et al., 1975; Hays, 1983; Mia et al., 1983, 1987, 1988a). These cellular ultrastructural events are thought to occur through ADH V_2 receptors coupled to the activation of adenylate cyclase, an increase in cAMP and the activation of protein Kinase A (Handler and Orloff 1973, 1981; Schlondorff and Levine, 1985). Amphibian epithelia also contain an ADH V_1 receptor coupled to phosphoinositide metabolism and inositol triphosphate release (Yorio et al., 1985; Yorio and Satumtira, 1989), which appears to play a functional role in the overall scheme of transepithelial aqueous flow possibly through the activation of PKC. It has been shown that mezerein (MZ), a non-phorbol activator of PKC, increased transepithelial water flow when added to the mucosal surface. Although the magnitude of water flow was less, and occurred over a longer period as compared to ADH stimulated tissues, the response was reminiscent to that seen with hormone (Yorio and Satumtira, 1989). A series of ultrastructural experiments also revealed that this enhanced water flow induced by MZ was indeed correlated with the propagation of apical microvilli and the change in the cellular distribution of PKC isozymes as determined by immunogold localization techniques (Mia et al., 1991b, 1992). It has been proposed by our laboratory that part of the initiation of transepithelial water flow by ADH involves V_1 receptors and the activation of PKC. The water channels (aggrephores) are likely transported from the cytosol to the apical membrane domain through an involvement of PKC. Our observations involving the role of PKC during enhanced transepithelial water transport correlated with cytomorphological changes and

concurrent apical membrane surface remodeling, suggest that PKC may play an integral role in the phenomenon of membrane recycling.

The process of endocytosis in amphibian bladder tissues has been described (Muller and Kachadorian, 1984; Ding et al., 1985; Harris et al., 1986; Coleman et al., 1987). Following stimulation of tissues by hormone, the membrane permeability to water declines with time and the tissue looses its responsiveness to ADH. During this period, membrane recycling takes place resulting in a membrane remodeling and a return of the apical membrane to the normal unstimulated state. During this membrane restoration process it is assumed that water channels are retrieved by endocytosis. It has been predicted that the internalized membranes contain intact particles aggregates retrieved during endocytosis. Several studies on endocytosis, using amphibian urinary bladders, have shown evidence of membrane retrieval of intact particles aggregates using specific protein markers as identification of aggregate protein (Harris et al., 1986). Additional evidence for retrieval of water channels had come from ultrathin section and freeze fracture techniques using selectively labeled colloidal gold and horseradish peroxidase as tracers to localize membrane particle aggregates (Coleman et al., 1987). More recently, it has been shown that endocytosed membrane vesicles retain their permeability to water following ADH action (Brown, 1989). While these studies involve the cellular localization of retrieved aggrephores following withdrawal of ADH, there are no studies on surface changes during this process nor time-course studies reported. Our present time-course studies provide insight into the membrane surface behavior following withdrawal of ADH or MZ. During this process, granular epithelial cell membranes tend to invaginate toward the cellular interior as an initial response to ADH or MZ withdrawal. This could result from the loss of membrane permeability to water, or as an initial cytosolic signal to begin the retrieval process.

Since transepithelial water flow is maintained during the period, it is highly unlikely that this internalization process is initiated by changes in membrane permeability or dissipation of the osmotic gradient. The membrane internalization process appears to enter into transitional stages resulting in the loss of the surface microstructures (microvilli) prior to the restoration of the apical membrane to one predominantly containing microridges. The restoration of apical membranes is correlated with a decrease in transepithelial water transport. It is also noteworthy that even when hormone is continually present there appears to be a down-regulation of membrane permeability and an internalization of membrane water channels. Therefore, additional unknown mechanisms may act to bring about a return of the membrane to its normal state. The present observations indicate and reinforce our previous observations that protein kinase C may be involved in the insertion of membrane water channels during exocytosis, whereas the process of endocytosis may be mediated by other cellular events. Further research in the mechanisms regulating retrieval of water channels is necessary so that a complete picture of membrane recycling and its regulation may be presented. Such a story could lead to suggestive measures to improve or enhance water reabsorptive processes in the kidney. Such measures will maximize water retention during periods of water deprivation as may be experienced by soldiers in a desert environment.

REFERENCES

Asotra, K. and Macklin, W.B. 1993. Use of affinity-purified and protein G-purified antibodies to study protein kinase C isozyme expression in oligodendrocytes. Focus, 15, 94-98.

Ausiello, D.A., Skorecki, K.L., Verkman, A.S. and Bonventre, J.V. 1987. Vasopressin

signaling in kidney cells. Kidney Int. , 31, 521-529.

Bentley, P.J. 1958. The effects of neurohypophysial extracts on water transfer across the wall of the isolated urinary bladder of the toad, *Bufo marinus*. J. Endocrin., 17, 201-209.

Bradford, U. 1976. A rapid and sensitive method for the quatification of microgram quantities of protein utilizes the principle of protein-dye binding. Ann. Biochem., 72, 248-254.

Brodsky, F.M. 1988. Living ith clatharin: Its role in intracellular membrane traffic. Sci., 242, 1396-1402.

Brown, D. 1989. Vesicle recycling and cell-specific function in kidney epithelial cells. Annu. Rev. Physiol., 51, 771-784.

Brown, D., Verkman, A. S., Skorecki, K. and Ausiello, D.A. 1990. The cellular action of Antidiuretic Hormone. Meth. in Enzymology 191, 551-571.

Cammarata, P.R., Fan, W., Jin, Y. and Yorio, T. 1993. Protein kinase C activity and its relation ship to myo-inositol uptake during hyperglycemic conditions in cultured bovine lens epithelial cells. Current Eye Res. , 12, 403-412.

Candia, O., Mia, A.J. and Yorio, T. 1993. Influence of filter supports on transport charateristics of cultured A6 kidney cells. Am. J. Physiol., 265 (Cell Physiol. 34), C1479-C1488).

Chevalier, J., Bourguet, J. and Hugon J.S. 1974. Membrane associated particles: distribution in frog urinary bladder epithelium at rest and after oxytocin treatment. Cell Tiss. Res. , 152, 129-140.

Coleman, R.A., Harris, W. Jr., and Wade, J.B. 1987. Visualization of endocytosed markers in freeze-fracture studies of toad urinary bladder. J. Histochem. Cytochem., 35, 1405-1414.

Davis, W.L., Goodman, B.P., Schuster, R.J., Rasmussen, H. and Martin, J.H. 1974. Effects of cytochalasin B on the response of toad urinary bladder to vasopressin. J. Cell Biol., 63, 986-997.

Davis, W.L., Jones, R.G., Ciumei, J., Knight, P.C. and Goodman, D.B. 1982. Electron-microscopic and morphometric study of vesiculation in the epithelial cell layer of the toad urinary bladder. Cell Tissue Res., 225, 619-631.

DiBona, D.R., Civan, M.M. and Leaf, A. 1969. The cellular specificity of the effect of vasopressin on toad urinary bladder. J. Membr. Biol., 1, 79-91.

DiBona, D.R. 1978. Direct visualization of epithelial morphology in the living amphibian urinary bladder. J. Membr. Biol., 400, 45-70.

DiBona, D.R. 1981. Vasopressin action of the conformational state of the granular cell in the amphibian urinary bladder. In Epithelial Ion and Water Transport. J. Cardiovasc. Pharm., 8, 23-528.

Ding, G., Franki, N. and Hays, R.M. 1985. Evidence of cycling of aggregate-containing tubules in toad urinary bladder. Biol. Cell, 55, 213.

Dratwa, M., LeFurgey, A. and Tisher, C.C. 1979. Effect of vasopressin and serosal hypertonicity on toad urinary bladder. Kidney Int., 16, 695-703.

Gronowicz, G., Massur, S.K. and Holtzman, E. 1980. Quantitative analysis of exocytosis and endocytosis in the hydroosmotic response of toad urinary bladder. J. Membr. Biol. , 52, 221-235.

Grynkiewicz, G., Poenie, M. and Tsien, R.Y. 1985. A new generation of Ca^{2+} indicators with greatly improved fluorescence properties. J. Biol. Chem., 260, 3440-3450.

Handler, J.S. and Orloff, J. 1973. The mechanism of action of anti-diuretic hormone. Handbook of Phys., 8, 791-814.

Handler, J.S. and Orloff, J. 1981. Antidiuretic hormone. Ann. Rev. Physiol., 43, 611-624.

Hardy, M.A. and DiBona, D.R. 1982. Microfilaments and the hydro-osmotic action of vasopressin in toad urinary bladder. Am. J. Physiol., 243, C200-C204.

Harris, H.W., Wade, J.B. and Handler, J.S. 1986. Fluorescent markers to study membrane retrieval in ADH treated toad urinary bladder. Am. J. Physiol., 251, C274.

Hays, R. M, Bourguet, J., Satir, B.H., Franki , N. and Rapaport, J. 1982. Retention of antidiuretic hormone-induced particle aggregates by luminal membranes separated from toad bladder epithelial cells. J. Cell Biol. 92: 237-241.

Hays, R.R. 1983. Alteration of luminal membrane structure by antidiuretic hormone. Am. J. Physiol., 245, C289-C296.

Hays, R. M., Chevalier, J., Gobin, R. and Bourget, J. 1985. Fusion images and intramembrane particle aggregates during the action of antidiuretic hormone. A rapid freeze study. Cell Tissue Res., 240, 433-439.

Humbert, F., Montesano, R., Grosso, A., DeSousa, R.C. and Orci, L. 1977. Particle aggregates in plasma and intracellular membranes of toad bladder (granular cells). Experimentia, 33, 1364.

Ito, T., Tanaka, T., Yoshida, T., Oneda, K., Ohta, H., Hagiwara, M., Ito, Y., Ogwa, M., Saito, H. and Hidaka, H. 1988. Immunocytochemical evidence for translocation of protein kinase C in human megakaryoblastic leukemic cells: Synergistic effects of Ca^{2+} and activators of protein kinase C on the plasma membrane association. J. Cell Biol., 107, 929-937.

Jaken, S., Leach, K. and Klauck, T. 1989. Association of type 3 protein kinase C with focal contracts in rat embryo fibroblasts. J. Cell Bio., 109, 697-704.

Kachadorian, W.A., Casey, C. and DiScala, V.A. 1977. Time course of ADH-induced

intramembrane particle aggregation in toad urinary bladder. Am. J. Physiol. 234, F461-F465.

Kachadorian, W.A., Muller, J., Rudich, S. and DiScala, V.A. 1978. Time course of ADH-induced intramembrane particle aggregation in toad urinary bladder. Am. J. Physiol., 234, F461.

Leach, K.L., Ponus, E.A., Ruff, V.A., Jaken, S. and Kaufmann, J. 1989. Type 3 protein kinase C localization to the nuclear envelope of phorbol ester-treated NIH 3T3 cells. J. Cell Biol., 109, 685-695.

LeFurgey, A. and Tisher, C.C. 1981. Time course of vasopressin-induced formation of microvilli in granular cells of toad urinary bladder. J. Membr. Biol., 61, 13-19.

Mia, A.J., Tarapoom, N., Carnes, J. and Yorio, T. 1983. Alteration in surface substructure of frog urinary bladder by calcium ionophore, verapamil and antidiuretic hormone. Tissue & Cell, 15, 737-748.

Mia, A.J., Oakford, L.X., Torres, L., Herman, C. and Yorio, T. 1987. Morphometric analysis of epithelial cells of frog urinary bladder. I. Effect of antidiuretic hormone, calcium ionophore (A23187) and PGE_2. Tissue & Cell, 19, 437-450.

Mia, A.J., Oakford, L.X., Moore, T.M., Chang, P.H. and Yorio, T. 1988a. Morphometric analysis of epithelial cells of frog urinary bladder. II. Effect of ADH, Calcium Ionophore (A23187) and verapamil on isolated and dissociated cells. Tissue & Cell, 20, 19-33.

Mia, A.J. Oakford, L.X. and Yorio, T. 1988b. Effect of verapamil on cytoplasmic distribution of granules and microfilaments in amphibian urinary bladder. Proc. Elect. Microscopic. Soc. Am., 46, 324-325.

Mia, A.J., Oakford, L.X. and Yorio, T. 1989a. Alterations in surface substructures and degranulation of subapical cytoplasmic granules by mezerein (MZ) in toad urinary

bladder epithelia. Proc. Elect. Microscopic. Soc. Am., 47, 916-917.

Mia, A.J., Oakford, L.X. and Yorio, T. 1989a. Modulation of cytoskeletal organization and cytosolic granule distribution by verapamil in amphibian urinary bladder. J. Cell Biol., 107, 772.

Mia, A.J., Oakford, L.X., Cammarata, P. and Yorio, T. 1991a. Modulation of cytoskeletal organization and cytosolic granule distribution by verapamil in amphibian urinary epithelia. Tissue & Cell, 23, 161-171.

Mia, A.J., Oakford, L.X. and Yorio, T. 1991b. Role of PKC isozymes in water transport in toad urinary bladder. Proc. Elect. Microscopic. Soc. Am., 49, 302-303.

Mia, A.J., Oakford, L.X., Thompson, P.D. and Yorio, T. 1992. Role of PKC isozyme III (alpha) in water transport in amphibian urinary bladder. Proc, Elect. Microscopic. Soc. Am., 50, 796-797.

Mia, A.J., Oakford, L.X., Yancy, H.F., Davidson, A.D. and Yorio, T. 1993a. Evidence of endocytosis in toad urinary bladders as revealed by SEM. FASEB J., 7, A577.

Mia, A.J.., Oakford, L.X., Hayes, S.C., Davidson, A.D.. and Yorio, T. 1993b. Membrane dynamic during endocytosis in toad urinary bladders as visualized by SEM. Scanning 15 Suppl III, 110-111.

Mia, A.J., Davidson, A.D., Oakford, L.X. and Yorio, T. 1993c. SEM studies of membrane endocytosis in toad urinary bladders following withdrawal of mezerin. Proc. Microscopy Soc. Am., 474-475.

Mia, A.J., Oakford, L.X. and Yorio, T. 1994. Surface membrane remodeling following removal of vasopressin in amphibian urinary bladder. Tissue & Cell, 26, 189-201.

Mills, J.J. and Malick, L.E. 1978. Mucosal surface morphology of the toad urinary bladder. Scanning electron microscopic study of the natriferic and hydro-osmotic response to vasopressin. J. Cell Biol., 77, 598-610.

Mochly-Rosen, D., Hendrick, C.J., Cheever, L., Khaner, H. and Simpson, P.C. 1990. A protein kinase C isozyme is translocated to cytoskeletal elements on activation. Cell Regul., 1, 693-706.

Muller, J. and Kachadorian, W.A. 1984. Aggregate-carrying membranes during ADH stimulation and washout in toad bladder. Am. J. Physiol., 247, C90-C98.

Pearl, M. and Taylor, A. 1983. Actin filaments and vasopressin-stimulated water flow in a toad urinary bladder. Am. J. physiol., 245, C28-C39.

Pearse, M.F. and Crowther, R.A. 1987. Structure and assembly of coated vesicles. Annu. Rev. Biophys. Chem., 16, 49-68.

Perkins, F.M. and Handler, J.S. 1981. Transport properties of toad kidney epithelia in culture. Am. J. Physiol., 241 (Cell Physiol. 10), C154-C159.

Schlondroff, D. and Levine, S.D. 1985. Inhibition of vasopressin-stimulated water flow in toad urinary bladder by phorbol myristate acetate, dioctanoylglycerol, and RHC-80267. J. Clin. Invest., 76, 1071-1078.

Schlondorff, D. and Satriano, J.A. 1985. Interactions of vasopressin, cAMP, and prostaglandins in toad urinary bladder. Am. J. Physiol., 248, F454-F458.

Schmid, S.L. 1992. The mechanism of receptor-mediated endocytosis: More questions than answers. BioEssays, 14, 589-596.

Simboli-Campbell, M., Gaynon, A., Welsh, J. and Franks, D.J. 1993. Analysis of PKCε in renal cells. Focus, 15, 12-15.

Smart, E.J., Ying, Y.S., Kamen, B.A. and Anderson, R.G.W. 1994. Protein kinase C activators prevent receptor-mediated potocytosis by inhibiting internalization of caveolae. Mol. Biol. Cell, 4, 435a.

Spinelli, F., Grosso,A. and DeSousa, R.C. 1975. The hydrosomotic effect of vasopressin: A scanning electron-microscope study. J. Membr. Biol. , 23, 139-156.

Stossel, T.P. 1994. The machinery of cell crawling. Sci. Am. 54-63.

Taylor, A., Mamelak, M., Reaven, E. and Maffly, R. 1973. Vasopressin: possible role of microtubules and microfilaments in its action. Sci., 181, 347-350.

Teitelbaum, I. and Straheim, A. 1990. AVP stimulates adenylcyclase and phospholipase C in reciprocal fashion in cultured RIMCT cells. Am. J. Physiol., 259, C693-C696.

Wade, J.B. 1978. Membrane structural specialization of the toad urinary bladder revealed by freeze-fracture technique. III. Location, structure and vasopressin dependence of intramembrane particles arrays. J. Membr. Biol., special issue, 281.

Wade, J.B., Stetson, D.L. and Lewis, J.A. 1981. ADH action: evidence for a membrane shuttle mechanism. Ann. N.Y. Acad. Sci., 322, 106-117.

Yorio, T., Henry, S., Hodges, D. and Caffrey, J.L. 1983. Relationship of calcium and prostaglandins in the antidiuretic hormone response. Boichem. Pharmacol., 32, 113-118.

Yorio, T., Royce, R., Mattern, J., Oakford, L.X. and Mia, A.J. 1985. Inhibition of hydro-osmotic response to vasopressin and hypertonicity by phenothiazines and W7 calmodulin antagonism. Gen. Pharmac., 164, 347-353.

Yorio, T. and Satumtira, N. 1989. Contribution of the vasopressin V_1 receptor to its hydro-osmotic response. Biol.Cell, 66, 7-12.

Yoshida, Y., Huang, F.L., Nakabayashi, H. and Huang, K.P. 1988. Tissue distribution and development expression of protein kinase C isozymes. J. Biol. Chem., 263, 9868-9873.

ACKNOWLEDGEMENT

The authors sincerely express their appreciation to the U.S. Army Medical Research and Development Command for supporting their research project on "Vasopressin Receptor Signaling and Cycling of Water Channels in renal Epithelia", tenured at Jarvis Christian College (an Historically Black College, HBCU), Hawkins, Texas and at the University of North Texas Health Science Center at Fort Worth/ TCOM (a Majority Research Institution, MRI), Fort Worth, Texas. The authors also thank the student research participants for their excellent technical support during the course of the project.

KEY TO FIGURES

Figure 1. Schematic presentation of unstimulated (A), ADH or MZ stimulated (B) cells, and retrieved cells (C) following withdrawal of ADH or MZ. A, aggrephores, D, desmosomes, En, endocytosomes, Mi, membrane invagination, M, microtubules, Mf, microfilaments, N, nucleus, PKC, protein kinase C enzyme localized with protein A-gold particles.

Figure 2. Schematic representation of experimental set-up of toad urinary bladder as a sac.

Figure 3. SEM of control toad urinary bladder tissue retained in Ringer's solution under an imposed osmotic gradient for 10 min showing apical plasma membrane predominantly containing microridges (arrows). X2,000.

Figure 4. SEM of toad urinary bladder tissue stimulated with 100mU/ml ADH for 10 min showing propagation of numerous microvilli (arrows) over the apical plasma membrane surface. X2,000.

Figure 5. SEM of toad urinary bladder tissue stimulated with MZ 10^{-6}M for 10 min showing propagation of numerous microvilli (arrows) over the apical plasma membrane surface. X2,000.

Figure 6. SEM of control toad urinary bladder tissue retained in Ringer's solution for 60 min showing the presence predominant microridges (arrows) over the granular cell surface. X4,000.

Figure 7. SEM of toad urinary bladder tissue stimulated with 100mU/ml ADH for 60 min showing formation of microvilli (arrows) over the surface of the granular cells. X4,000.

Figure 8. SEM of toad urinary bladder tissue stimulated with MZ 10^{-6}M showing the formation of microvilli (arrows) over the granular cell surface. X4,000.

Figure 9. Histograms representing the percent of granual cells with microvilli in the control, ADH and MZ treated toad urinary bladder cells for 10, 30 and 60 min respectively.

Figure 10. SEM of A6 amphibian kidney cultured cells grown on a ICN filter support and retained in DMSO solution for 60 min for control showing the surface substructures containing microridges and the cellular junctions. X4,000.

Figure 11. SEM of A6 amphibian kidney cultured cells grown on a ICN filter support and stimulated with 100mU/ml ADH for 60 min showing cellular swelling and caving of the cellular junctions, and the propagation of numerous microvilli over the cell surface. X4,000.

Figure 12. SEM of A6 amphibian kidney cultured cells grown on a ICN filter support and stimulated with MZ 10^{-6}M for 60 min showing the formation of microvilli over the cell surface. X4,000.

Figure 13. SEM of A6 amphibian kidney cultured cells grown on a ICN filter support and stimulated with ADH plus MZ for 60 min showing the formation of numerous microvilli over the cell surface and tissue swelling. X4,000.

Figure 14. TEM of control toad urinary bladder tissue retained in Ringer's solution for 10 min under an imposed osmotic gradient showing the general cytoplasmic composition, subapical secretory granules (arrows) and the basolateral membrane with little membrane infoldings. X12,800.

Figure 15. TEM of control toad urinary bladder tissue retained in Ringer's solution for 60 min under an imposed osmotic gradient showing the loss of heterochromatins and the general density of nuclei due to prolonged exposure to an osmotic gradient, and no loss of subapical secretory granules (arrows). X5,600.

Figure 16. Freeze fracture replica of a control toad urinary bladder tissue fractured

across the apical plasma membrane and the cytoplasm showing the impressions of the secretory granules (arrows) and the apical membrane containing a thin distribution of intramembrane particles. X24,000.

Figure 17. TEM of toad urinary bladder sac exposed to MZ 10^{-8}M for 5 min showing a dense cytoplasm with numerous microfilaments, a few microtubules (short arrows) and mitochondria with altered cristae (long arrows). X27,000.

Figure 18. TEM of toad urinary bladder sac challenged with MZ 10^{-6}M for 5 min showing a partial loss of the secretory granules (short arrows) and the highly indented basolateral membranes (long arrows). X24,000.

Figure 19. TEM of toad urinary bladder sac treated with MZ 10^{-6}M for 60 min showing the loss of secretory granules and heterochromatins from the nuclei of these cells. These cells also showed significant swelling. X4,000.

Figure 20. TEM of 100mU/ml ADH challenged toad urinary bladder sac for 60 min showing the preservation of the subapical secretory granules (arrows) and the general cytoplasmic composition. X5,600.

Figure 21. Freeze fracture replica of ADH challenged tissue for 60 min showing the distribution of intact secretory granules in the subapical cytoplasm (arrows). X48,000.

Figure 22. Freeze fracture replica of ADH challenged tissue for 60 min showing the parallel and circular oriented rough ER membrane profiles (arrows). X27,000.

Figure 23. Freeze fracture replica of ADH challenged tissue for 60 min showing golgi body with enlarged cisternae associated with many large vesicles. X40,000.

Figure 24. Freeze fracture replica of control tissue retained in Ringer's solution for 60 min showing golgi body with small cisternae and fewer small vesicles as compared to ADH treated tissues as shown in Figure 23. X40,000.

Figure 25. Freeze fracture replica of toad urinary bladder tissue stimulated with 100

mU/ml ADH for 60 min showing membrane fusion event with typical stellar particle orientation (arrow). X96,000.

Figure 26. Freeze fracture replica of toad urinary bladder tissue stimulated with MZ 10^{-6}M for 60 min showing membrane fusion events with stellar particle orientation (arrow). X96,000.

Figure 27. Freeze fracture replica of toad urinary bladder tissue stimulated concurrently with ADH and verapamil showing the occurrence of membrane fusion event (arrow). X64,000.

Figure 28. Ultrathin section of toad urinary bladder tissue stimulated with MZ 10^{-6}M for 60 min showing immuno A-gold localization of protein kinase C isozyme II (20nm) in diffused cytoplasmic bodies (arrows). X48,000.

Figure 29. Ultrathin section of toad urinary bladder tissue stimulated with MZ for 60 min showing immnuo A-gold (10nm) localization of protein kinase C isozyme III in a diffused cytoplasmic body (arrow). X32,000.

Figure 30. Ultrathin section of toad urinary bladder tissue stimulated with ADH for 60 min showing immuno A-gold (20nm) localization of protein kinase C isozyme I with a large number of gold particles concentrated in a diffused cytoplasmic body (arrow). X54,000.

Figure 31. Ultrathin section of toad urinary bladder tissue stimulated with MZ for 60 min showing immuno A-gold (10nm) localization of protein kinase C isozyme III with a large number of gold particles concentrated over a diffused cytoplasmic body (short arrow) in association with many microfilaments (long arrows). X48,000.

Figure 32. Ultrathin section of toad urinary bladder tissue stimulated with MZ for 60 min showing immuno A-gold (20nm) localization of protein kinase C isozyme I in a diffused cytoplasmic body adjacent to a microvillus (arrow). X128,000.

Figure 33. Ultrathin section of toad urinary bladder tissue stimulated with MZ for 60 min showing immuno A-gold (20nm) localization of protein kinase C isozyme I within two adjacent microvilli (arrows). X48,000.

Figure 34. Ultrathin section of toad urinary bladder tissue stimulated with ADH for 60 min showing immuno A-gold (10nm) localization of protein kinase C isozyme III within a microvillus (arrow) shown in a cross-sectional view. X90,000.

Figure 35. Ultrathin section of toad urinary bladder stimulated with ADH for 60 min showing dual labeling of immuno A-gold (5nm for isozyme II, 20nm for isozyme I) localization of protein kinase C in a microvillus (arrow) at the apical membrane surface. X48,000.

Figure 36. Ultrathin sction of control toad urinary bladder tissue retained in Ringer's solution and exposed to 0.1% BSA and then to 10nm protein A-gold probes showing no specific labeling with gold particles. X60,000.

Figure 37. Phase contrast micrograph of A6 amphibian kidney cultured cells grown in monolayer on a microscope glass cover slip. X280.

Figure 38. Immunofluorescent detection of PKC isozyme III in ADH stimulated A6 amphibian kidney cells using FITC showing the presence of particulate structures. X700.

Figure 39. Immunofluorescent detection of PKC isozymes III in MZ stimulated A6 amphibian kidney cells using FITC showing the presence of particulate structures. X700.

Figure 40. Control A6 amphibian kidney cells exposed to 0.1% BSA and then to FITC showing little or no fluorescence. X280.

Figure 41. Histograms showing the significant distribution of gold particles associated with ADH and MZ treated toad urinary bladder tissue against the control tissue.

Figure 54. SEM picture of normal LLC-PK_1 porcine kidney cultured cells grown on Anocell filter support showing scattered microridges over the cell surfface. X3,500.

Figure 55. Increased intracellular calcium in LLC-PK_1 porcine kidney cultured cells following stimulation with 10^{-8} M ADH.

Figures 56 and 57. Shows the comparative effects on intracellular calcium mobilization in response to ADH and oxytocin in LLC-PK_1 kidney cultured cells.

Figure 58. The effect of the oxytocin antagonist peptide on the actions of ADH and oxytocin on calcium mobilization..

Figure 59. Dose-effect of ADH on intracellular calcium concentration in the presence of an oxytocin antagonist in LLC-PK_1 porcine kidney cultured cells.

Figure 60. Effects of ADH on the intracellular distribution of calcium before and after the administration of oxytocin antagonist in LLC-PK_1 porcine kidney cultured cells.

Figures 61 and 62. SEM of control toad urinary bladder sacs retained in Ringer's solution for 10 and 20 min respectively, showing the surface substructures as composed of continuous phases of microridges. X 4,000.

Figure 63. SEM of toad urinary bladder tissue showing the induction of surface invaginations (arrows) in the granular cells during a 5 min retrieval following withdrawal of ADH. X5,400.

Figure 64. SEM of MZ stimulated toad urinary bladder tissue showing the induction of surface invaginations (arrows) in the granular cells during 5 min retrieval following withdrawal of MZ. X3,000.

Figure 65. Graph represents the percentage of endocytosed granular cells in toad urinary bladder tissue stimulated by ADH and MZ as compared to control tissues.

Figure 66. SEM of MZ treated toad urinary bladder tissue for 10 min and retrieved for 30 min following withdrawal of MZ showing invaginations over the apical membrane

(arrows). X2,100.

Figure 67. SEM of toad urinary bladder sac stimulated with ADH for 10 min and retrieved for 10 min following withdrawal of ADH showing granular cells with surface invaginations (arrows). X2,000.

Figure 68. TEM of ADH stimulated toad urinary bladder sac showing a sectional view of the apical membrane invagination at 10 min retrieval following withdrawal of ADH. X30,000.

Figure 69. SEM of toad urinary bladder sac stimulated with ADH for 10 min and then retrieved for 20 min following withdrawal of ADH, showing endocytosis and restoration of apical membranes (arrows) involving many granular cells. X1,050.

Figure 70. SEM of toad urinary bladder sac stimulated with MZ for 10 min and then retrieved for 10 min following withdrawal of MZ showing endocytosed granular cells. X3,000.

Figure 71. TEM of toad urinary bladder cells stimulated with ADH for 15 min and then retrieved for 20 min following withdrawal of ADH showing deep invaginations with formation of vacuoles (arrows) and the displacement of nucleus. X15,000.

Figure 72. TEM of toad urinary bladder sac stimulated with ADH for 15 min and then retrieved for 20 following withdrawal of ADH showing the presence of coated vesicles (arrows) within the cytoplasm. X80,000.

Figure 73. Freeze fracture replica prepared from toad urinary bladder sac stimulated with ADH for 15 min showing the presence of coated vesicles (arrows) within the cytoplasm. X112,000.

Figures 74 and 75. Toad urinary bladder tissues stimulated with MZ 10^{-6} M for 15 min and then labeled with anti-PKC isozyme I and protein A-gold probes. Gold particles appear localized predominantly in association with coated vesicles indicating

association of PKC isozyme I with coated vesicles (arrows). X33,750.

Figure 76. Toad urinary bladder tissue stimulated with MZ 10^{-6} M for 15 min and then labeled with anti-PKC isozyme I and protein A-gold probes. Gold particles are shown to be associated with several coated vesicles (arrows) which indicate the association of PKC isozyme I with coated vesicles. These coated vesicles appear to show a pattern of migration from the apical membrane into the cytosol. X33,750.

Figure 77. Freeze fracture replica of toad urinary bladder tissue stimulated with ADH showing the presence of protocytosed caveolae (arrows) in a microfilament-rich cell. X67,000.

Figure 78. SEM of ADH stimulated toad urinary bladder sac for 15 min and then retrieved for 60 min following withdrawal of ADH showing the restoration of the apical membrane almost to a normal state as in the prehormone treated tissue. X700.

Figure 79. SEM of toad urinary bladder sac stimulated with MZ for 10 min and then retrieved for 30 following withdrawal of MZ showing the apical membrane restoration almost toa normal state except for few invaginations. X700.

Figure 80. SEM of toad urinary bladder sac stimulated with MZ and then retrieved for 60 min following withdrawal of MZ showing almost complete restoration of the apical membrane to a normal state. X700.

Figure 81. SEM of toad urinary bladder tissue showing the apical membrane restoration and the presence of a few invaginations at 30 min following withdrawal of ADH. X2,000.

Figure 82. SEM of toad urinary tissue treated with MZ for 10 min and then retrieved for 20 min following withdrawal of MZ showing details of membrane restoration and a gradual return of apical microridges. X8,000.

Figure 83. SEM of toad urinary bladder sac showing the gradual restoration of

microridges in an endocytosed pit at 30 min following withdrawal of ADH. X8,000.

Figure 84. Graph shows the comparative loss of water from the toad urinary bladder sacs following withdrawal of ADH while maintaining the osmotic gradient in the experimental sac. Measurements were made at 25, 45, 60 and 75 min.

RESEARCH CONTRIBUTIONS

Full-length Papers Published:

Candia, O., Mia, A. J. and Yorio, T. 1993. Influence of filter supports on transport characteristics of cultured A6 kidney cells. Am. J. Phisiol.

Mia, A.J., Oakford, L. X. and Yorio, T. 1994. Surface membrane remodeling following removal of vasopressin in toad urinary bladder. Tissue and Cell, 26(2): 189-201.

Mia, A.J., Oakford, L.X., Davidson, A. and Yorio, T. Protein kinase C isoforms and vasopressin-medicated water flow in toad urinary bladder. Tissue and Cell (In preparation).

Published Abstracts:

a) Mia, A.J., Oakford, L.X., and Yorio, T. 1992. Vasopressin-induced morphological changes in cultured amphibian A-6 kidney cells. FASEB J. 6(5): A957.

b) Mia, A.J., Oakford, L.X. and Yorio, T. 1992. Water permeability response to vasopressin (AVP) of A-6 cells grown on Anocell filter inserts. FASEB J. 6(5):A1194.

c) Mia, A.J., Oakford, L.X., and Yorio, T. 1992. Characteristics of Vasopressin V_1 and V_2 actions in cultured amphibian A-6 cells. Proc. 5th International Congress on Cell Biology, Madrid, Spain, 112.

d) Mia, A.J., Oakford, L.X., Thompson, P.D., and Yorio, T. 1992. Role of PKC isozyme III (alpha) in water transport in amphibian urinary bladder. MSA 50:796-797.

e) Mia, A.J., Oakford, L.X., and Yorio. 1992. Surface substructural changes of renal A-6 cells on filter supports following activation of PKC. Mol. Biol. Cell. 3,

228a.

f) Mia, A.J., Oakford, L.X., Finkley, A.E., Davidson, A.D., and Yorio, T. 1993. SEM studies of membrane recycling in Vasopressin-stimulated toad urinary bladders. Proc. Soc. Exptl. Biol. Med. 203,258.

g) Mia, A.J., Oakford, L.X., Yancy, H.F., Davidson, A.D., and Yorio, T. 1993. Evidence of endocytosis in toad urinary bladders as revealed by SEM. FASEB J. 7,A5770.

h) Mia, A.J., Oakford, L.X., Hayes, S.C., Davidson, A.D., and Yorio, T. 1993. Membrane dynamics during endocytosis in toad urinary bladders as visualized by SEM. Scanning, 15, Suppl III, 110-111.

i) Mia, A.J., Davidson, A.D., Oakford, L.X., and Yorio, T. 1993. SEM studies of membrane endocytosis in toad urinary bladders following withdrawal of Vasopressin. Microscopic Soc. Am. 474-475.

j) Mia, A.J., Gunter, S., Johnson, S., Franklin, J.L., Tuck, T., Gardner, D., and Yorio, T.1993. Immunofluorescent detection of PKC alpha in A-6 amphibian kidney cells. Mol. Biol. Cell, 4, 358a.

k) Mia, A.J., Robinson, C., Bolden, A., Davidson, A.D., Oakford, L.X., and Yorio, T. 1993. Membrane remodeling by endocytosis in toad urinary bladders under sustained osmotic gradient. Mol. Biol. Cell, 4, 430a.

l) Mia, A.J., Davidson, A.D., Robinson, C, Oakford, L.X. and Yorio, T. 1994. SEM studies of comparative membrane remodeling by endocytosis in toad urinary bladders following withdrawal of ADH and MZ. Microsc. Soc. Am., 52, 350-351.

m) Mia, A.J., Oakford, L.X. and Yorio, T. 1994. Possible association of PKC with coated vesicles in ADH stimulated toad urinary bladders. Mol. Biol. Cell, 5, 445a.

n) Yorio, T. and Mia, A.J. 1994. Vasopressin increase in intracellular calcium in cultured renal epithelia may be mediated through an oxytocin receptor. Mol. Biol. Cell, 5, 141a.

OTHER ACTIVITES

The following African-American undergraduate students at Jarvis Christian College received training in biomedical research and career enrichment with financial support from this research project under the supervision of Dr. Mia at Jarvis and Dr. Yorio at the University of North Texas Health Science Center at Fort Worth/TCOM:

Pamler Thompson - A Presidential Scholar at Jarvis graduated in May 1992, Summa Cum Laude, with chemistry as a major and biology as a minor. Pamler has enrolled in a Ph.D. program at the University of North Texas Health Science Center at Fort Worth to pursue a career in biomedicine under the supervision of Dr. Yorio.

Haile Yancy - Graduated from Jarvis in May 1994 with majors in biology/chemistry, and now pursuing a Ph.D. in Cell Biology at Howard University, Washington, D.C. Haile had received research training during his undergraduate program working with Dr. Yorio at the UNT Health Science Center and with Dr. Loy Frazier at Baylor College of Dentistry.

Alvin Finkley - Graduated in May 1994 with honors in chemistry and minor in biology. He received further training under the supervision of Dr. Yorio at the UNT Health Science Center and plans to attend graduate school to pursue a Ph.D. in Biomedical Sciences at the Health Science Center in Fort Worth.

Ina Swopes - Graduated in May 1993 with a minor in biology and a major in chemistry.

The following African American undergraduate students trained under the current grant will graduate in May 1995.

Shondola Hayes - A Presidential Scholar at Jarvis transferred to Washington State University in Pullman. She had received research training at New York and Princeton Universities and plans a carreer in dentistry upon graduation in May 1995.

Chasity Robinson - A Presidential Scholar at Jarvis majoring in biology and a minor in chemistry. Plans to pursue a career in pharmacology. She received research training at the UNT Health Science Center under the supervision of Dr. Yorio and received further training in biomedicine at Indiana University, Bloomington under Dr. Kaufman's direction working on molecular biological techniques.

Kristi Henderson - A Presidential Scholar at Jarvis majoring in biology and a minor in chemistry. She plans a career in biomedicine. Has received research training in genetic finger printing and PCR techniques at the UNT Health Science Center under the supervision of Dr. Dzandu.

Tashara Tuck - An honor student at Jarvis majoring in biology with a minor in chemistry. She has received research training in Confocal Microscopy at Baylor College of Dentistry working with Drs. Frazier and Wong.

Julia Franklin - An honor student at Jarvis majoring in chemistry with a biology minor will graduate in May 1996.

Crystal Woods - Major in biology and minor in chemistry is making steady progress in her studies.

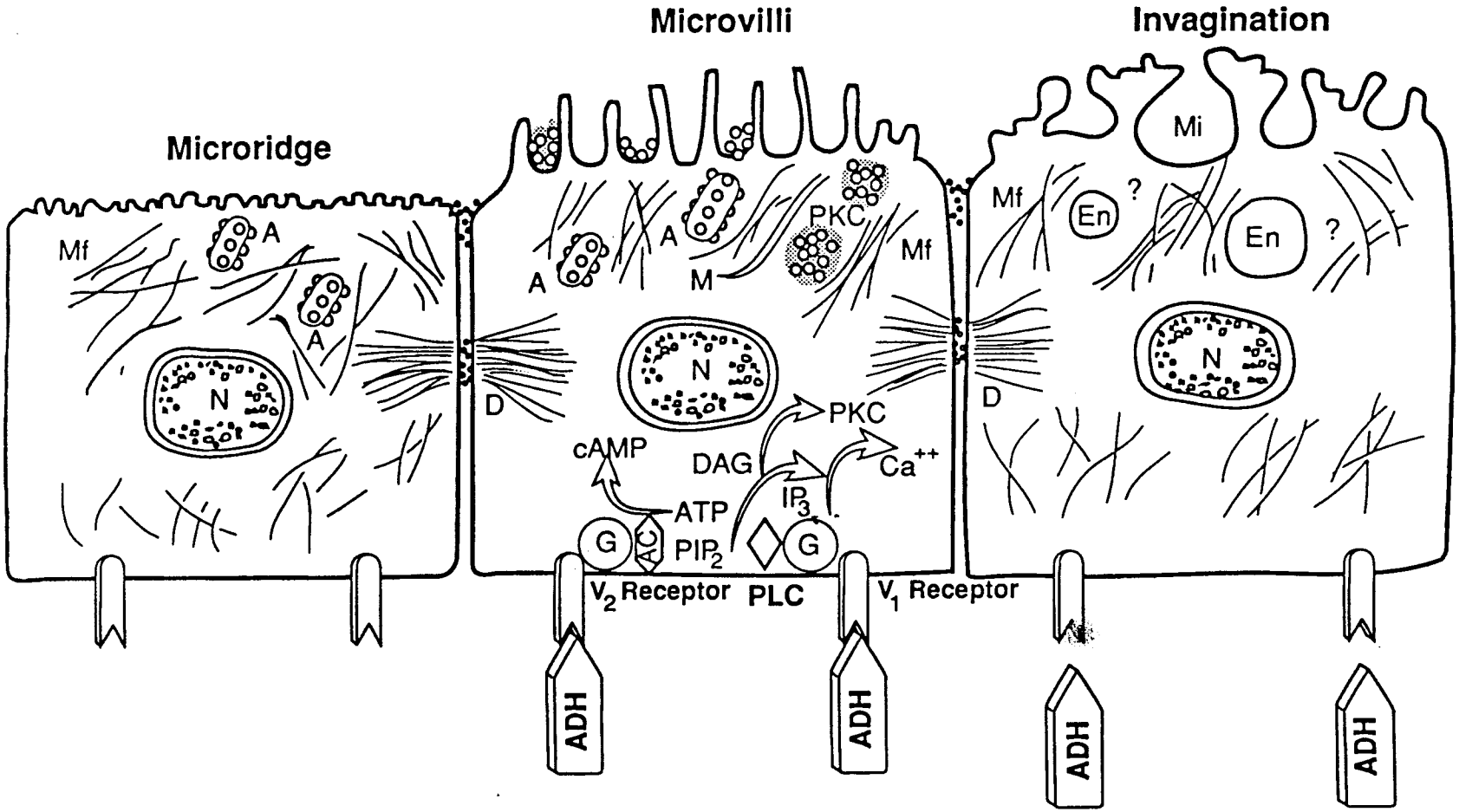
Microridge
Microvilli
Invagination
Mf
A
N
D
M
PKC
cAMP
DAG
ATP
PIP2
IP3
Ca++
G
V2 Receptor
PLC
V1 Receptor
ADH
Mi
En
?
(A) Unstimulated Cell
(B) Exocytosis
(C) Endocytosis

Figure 1

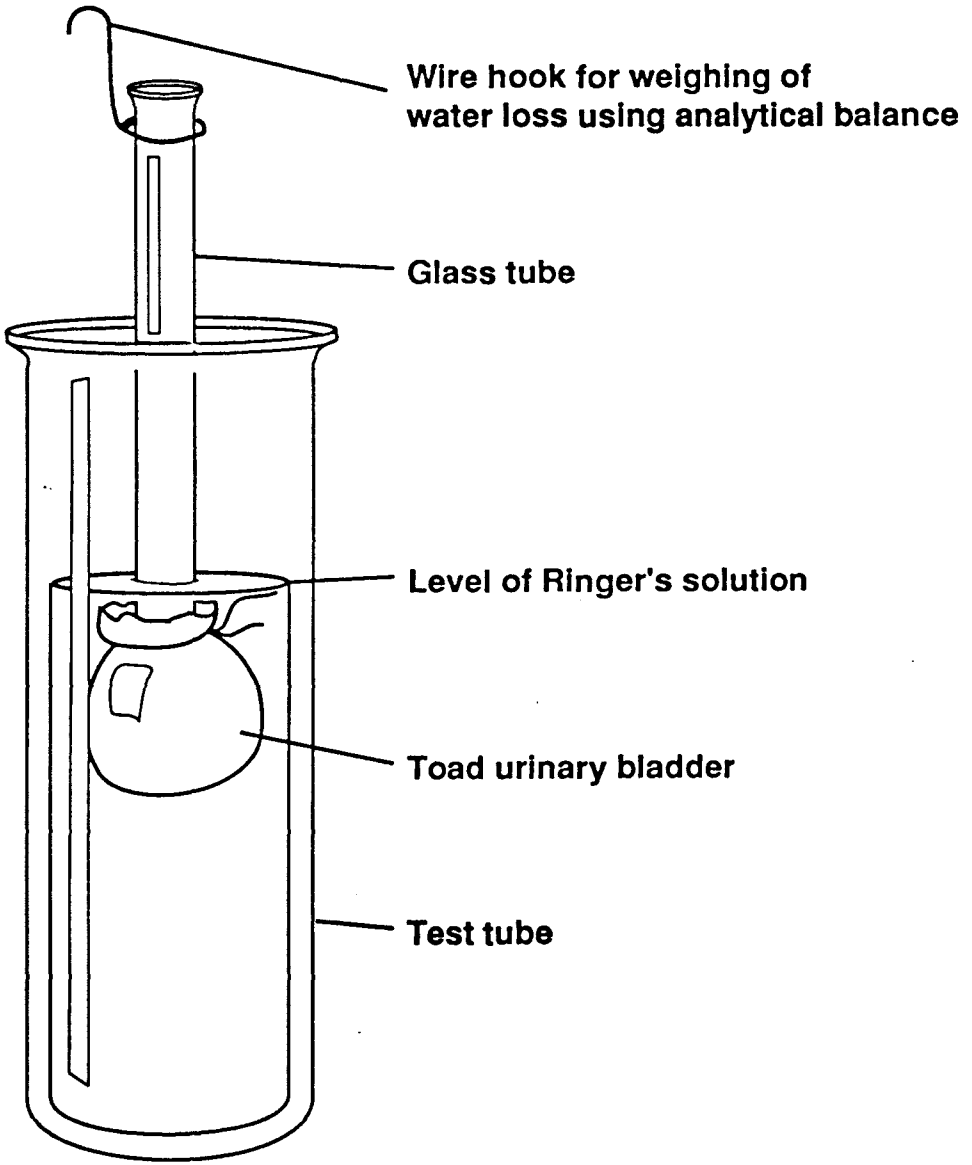
Wire hook for weighing of
water loss using analytical balance
Glass tube
Level of Ringer's solution
Toad urinary bladder
Test tube

Figure 2


3


4


5

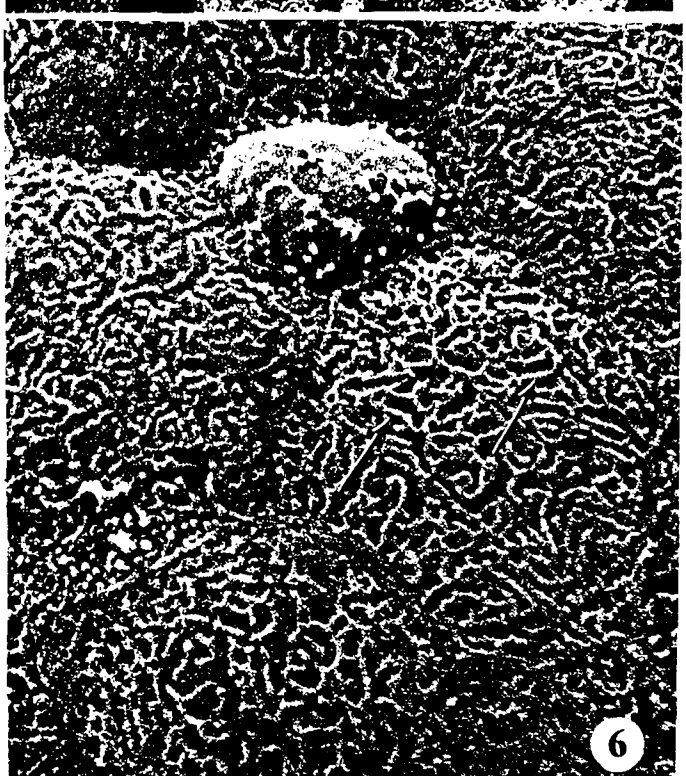
6

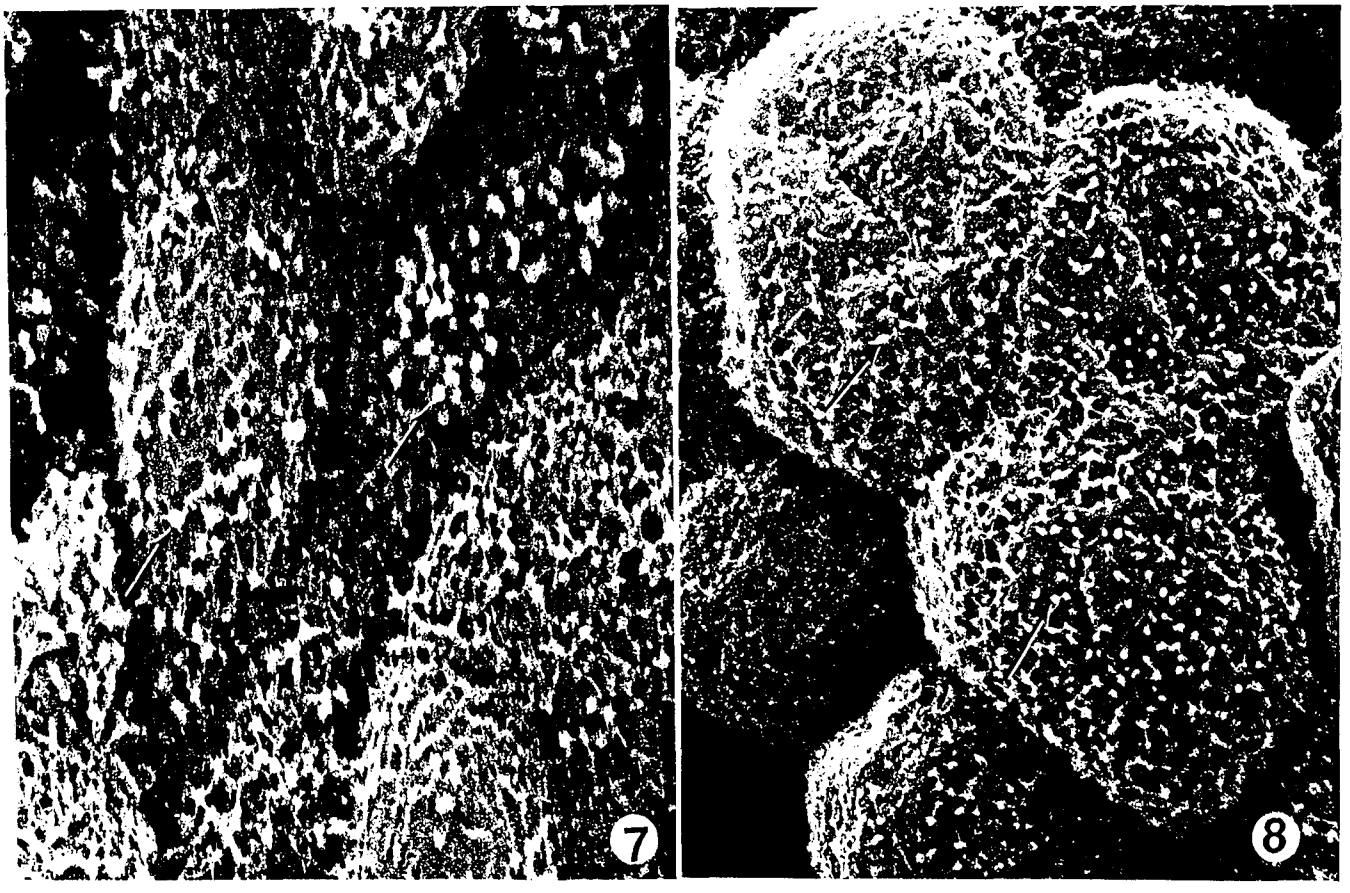

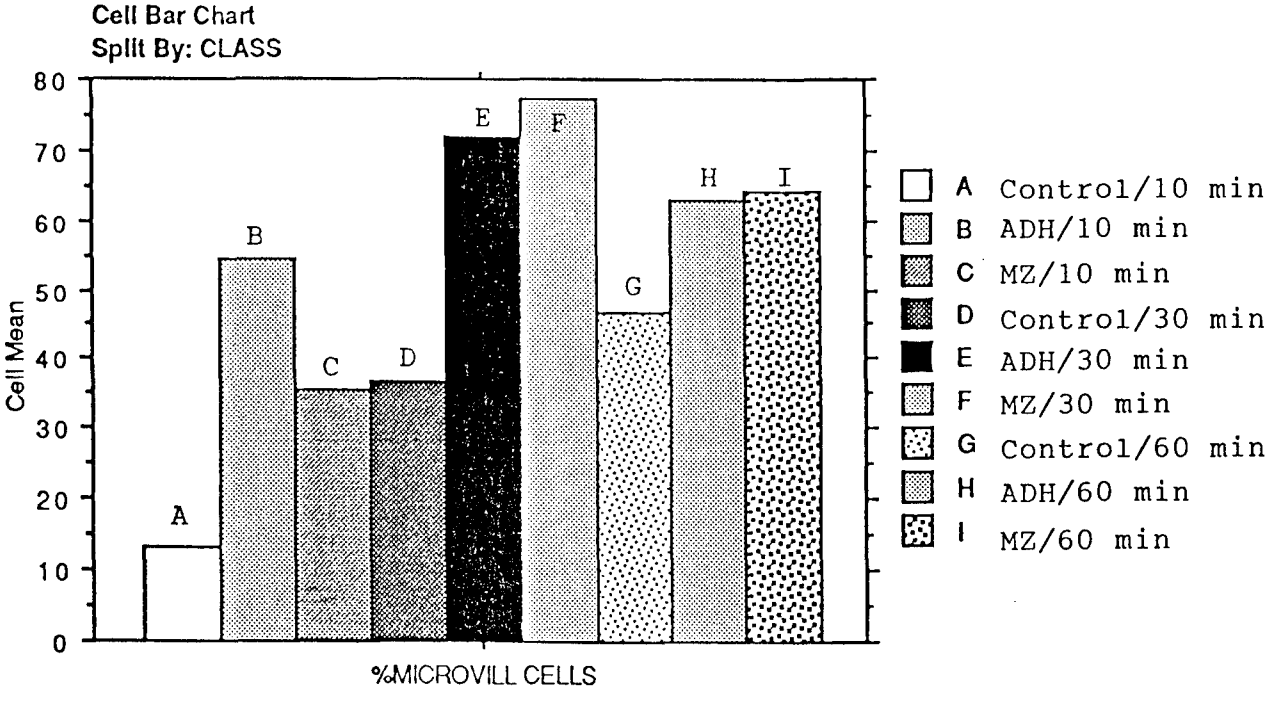

Histograms represent percent of cells showing microvilli in the control, ADH and MZ treated tissues at 10, 30 and 60 min.

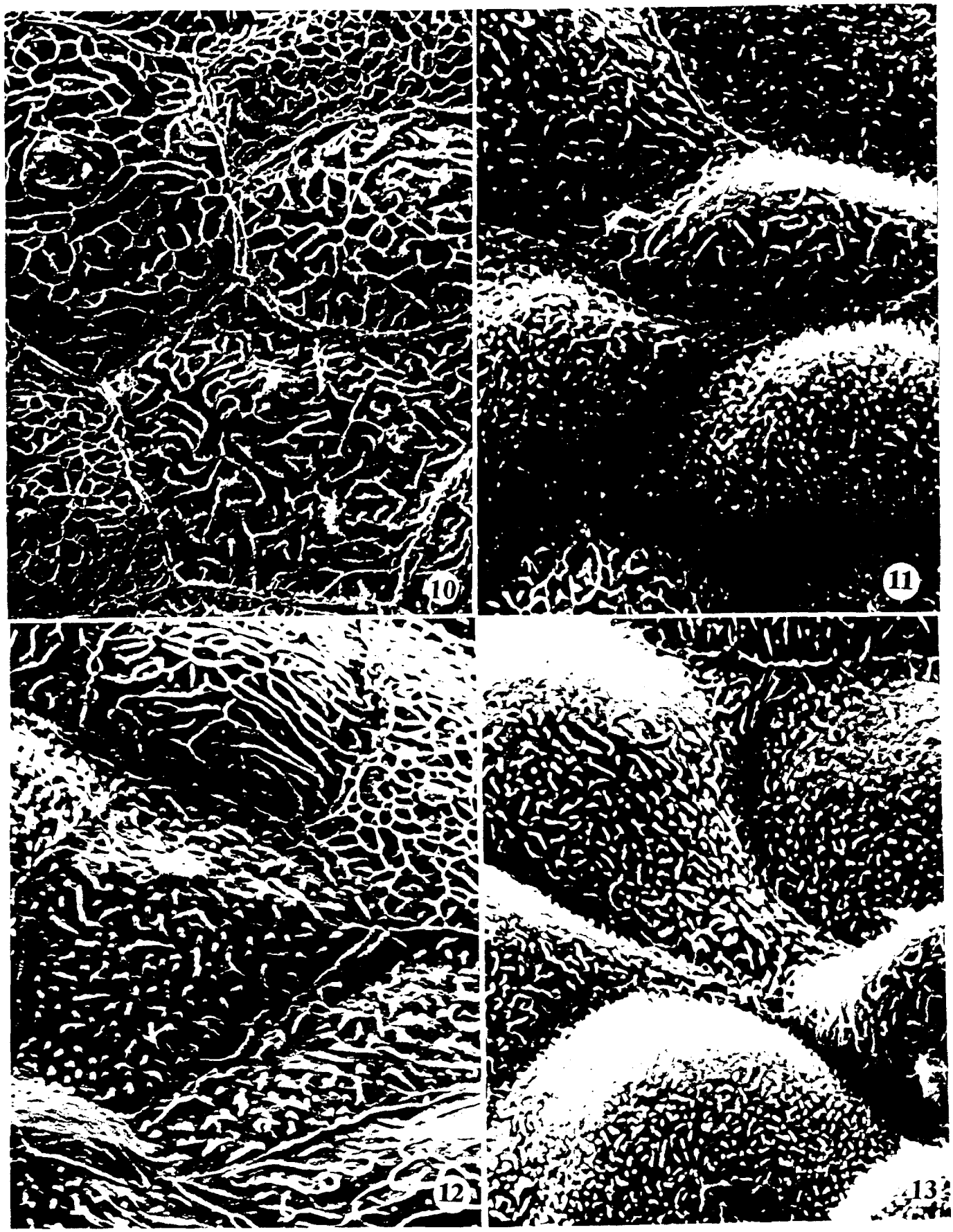
10
11
12
13


14


15


16

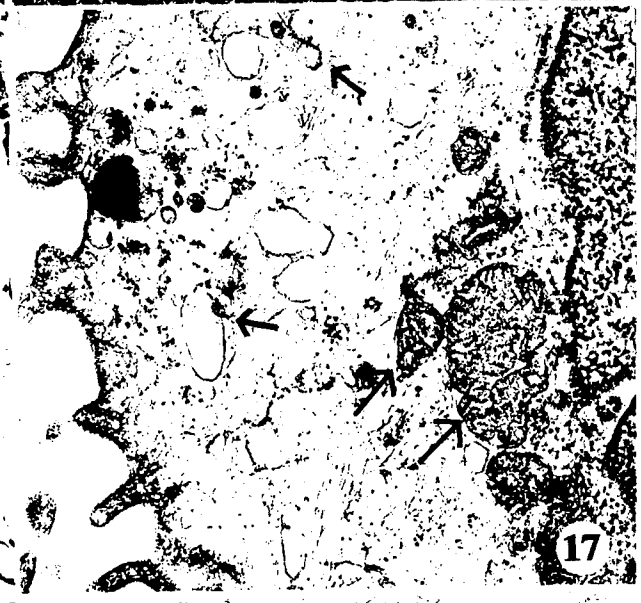
17


18


19


20

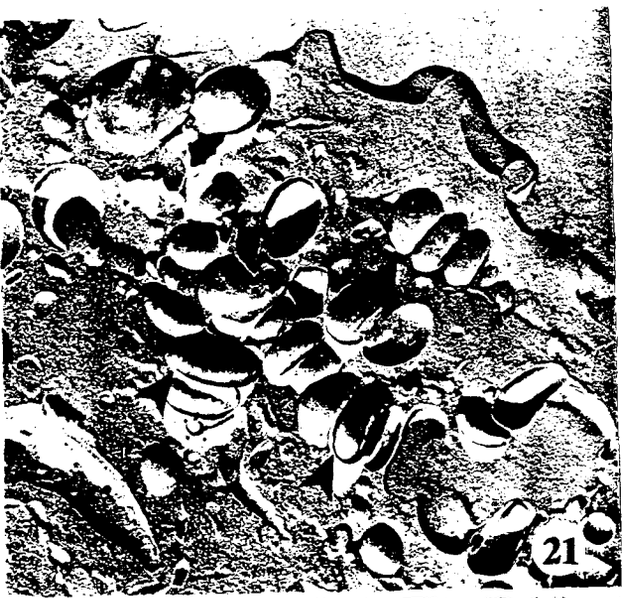
21

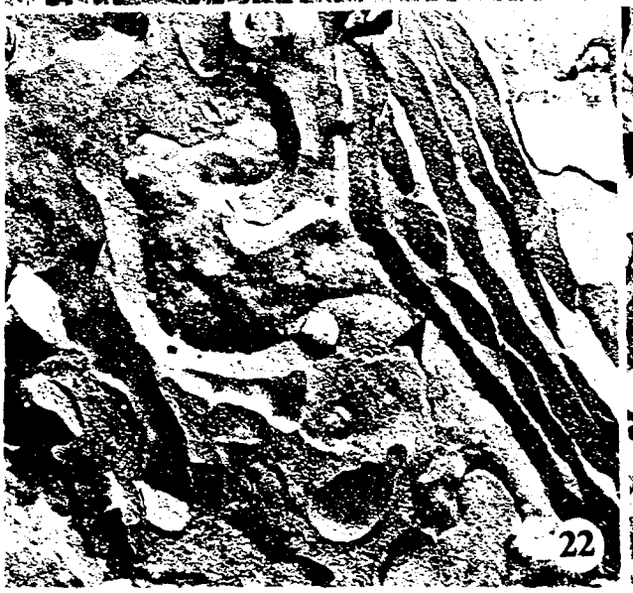
22


23

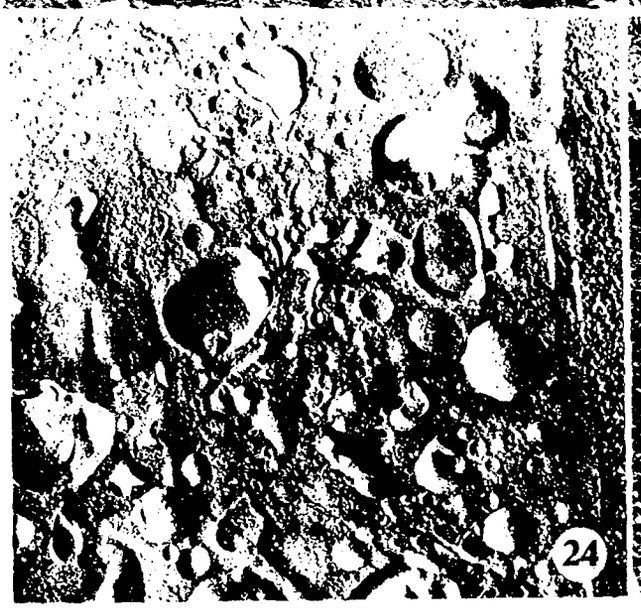
24


25

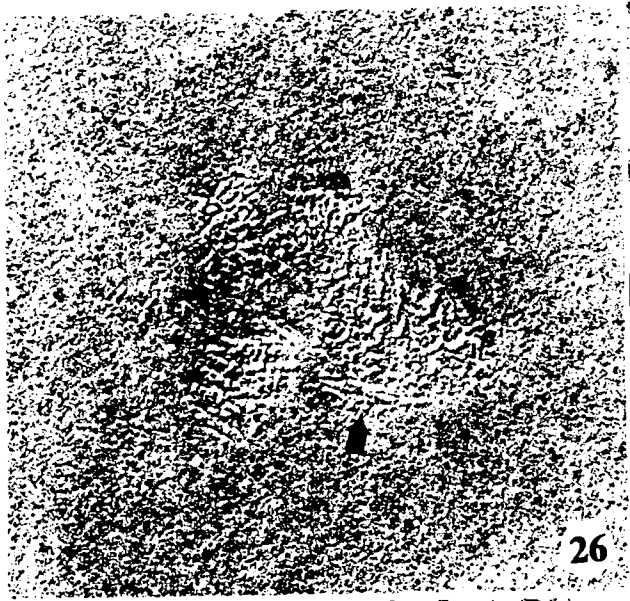
26

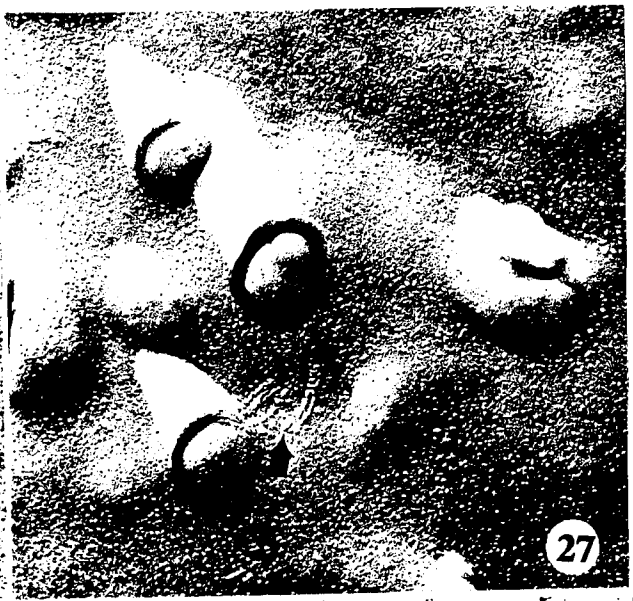
27

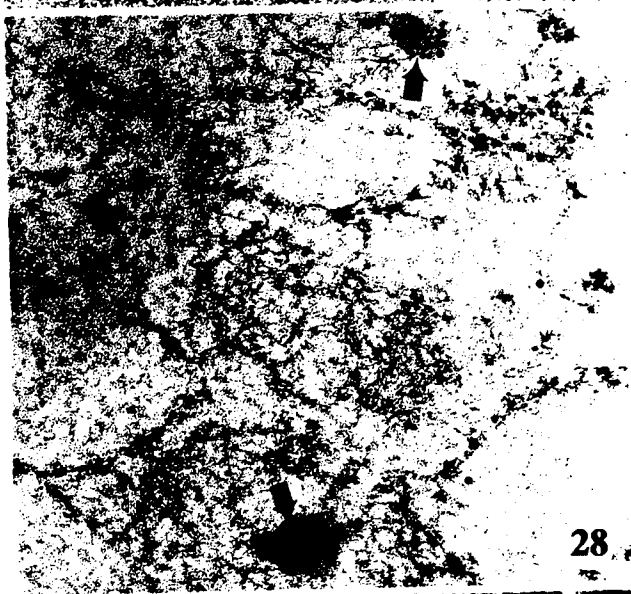
28

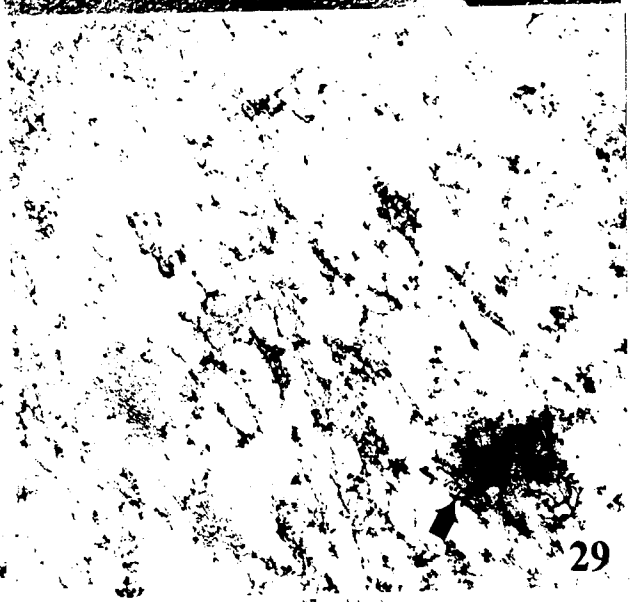
29

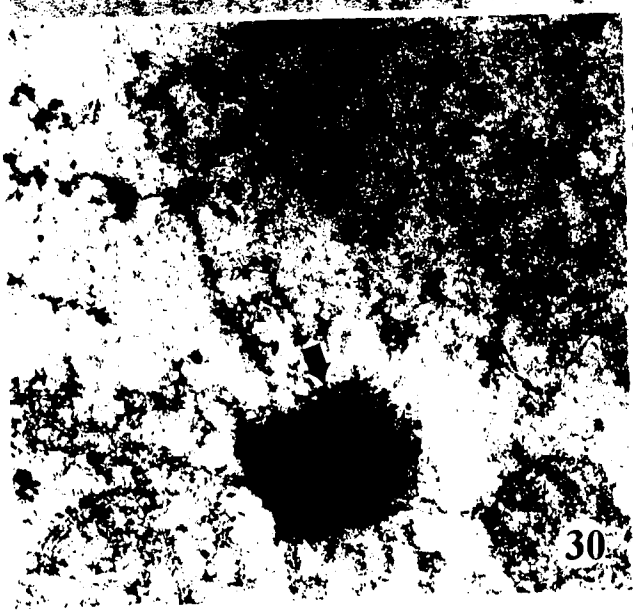
30


31

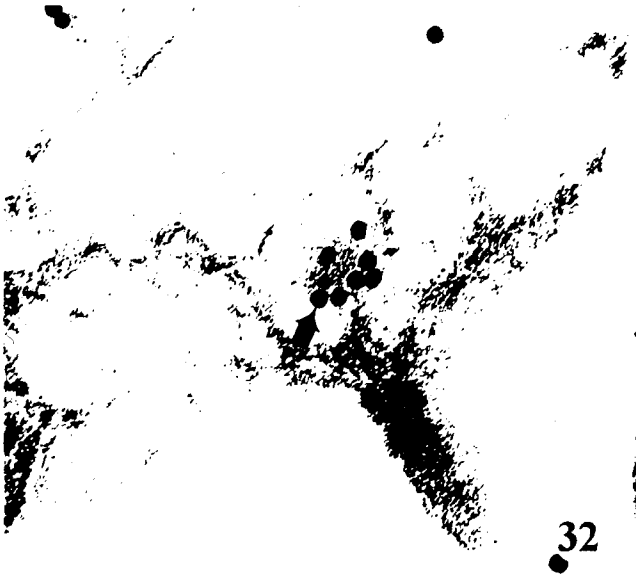

32

33

34

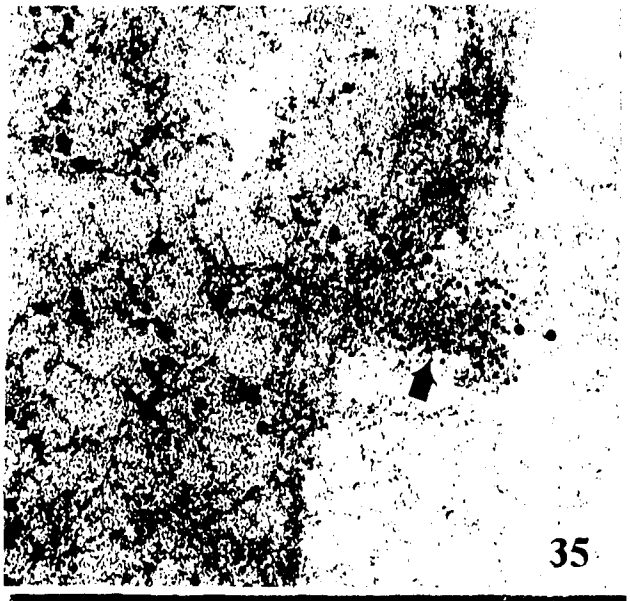

35

36

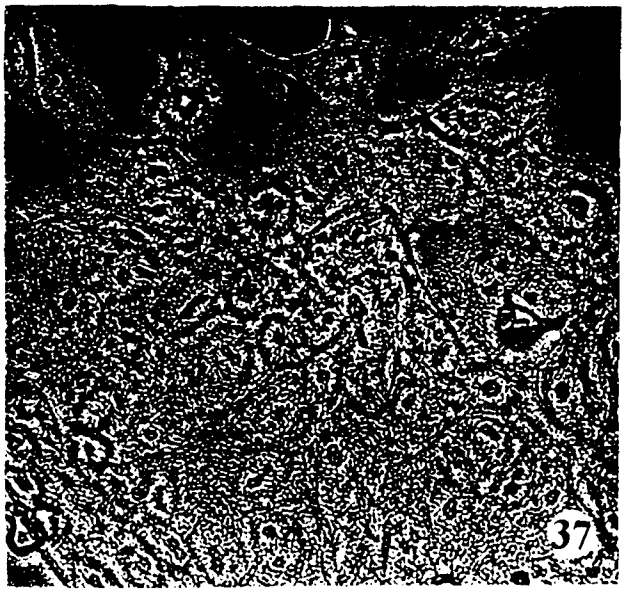

37

38

39

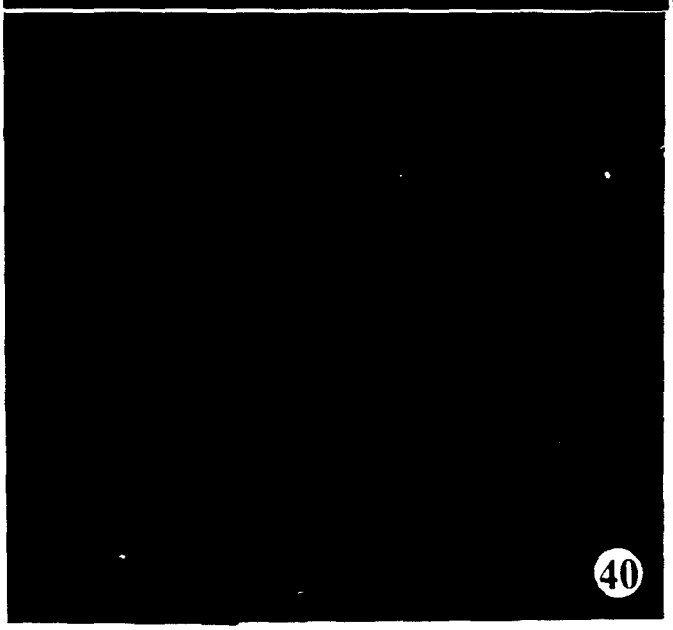

40

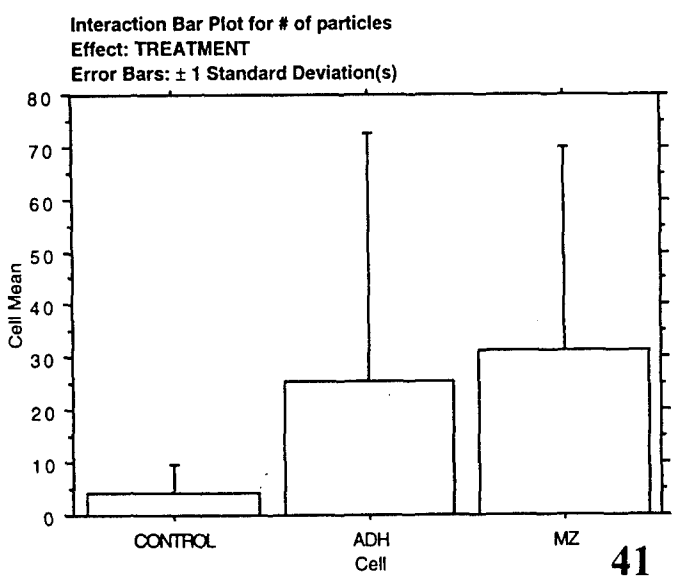
Interaction Bar Plot for # of particles
Effect: TREATMENT
Error Bars: ± 1 Standard Deviation(s)
Cell Mean
80
70
60
50
40
30
20
10
0
CONTROL
ADH
MZ
Cell

41

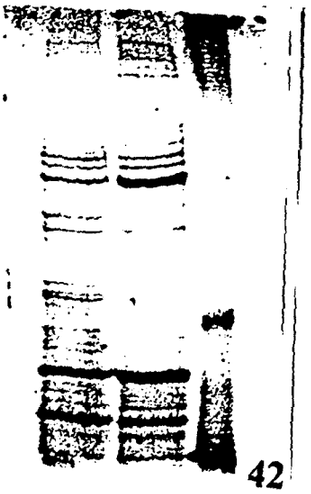

42

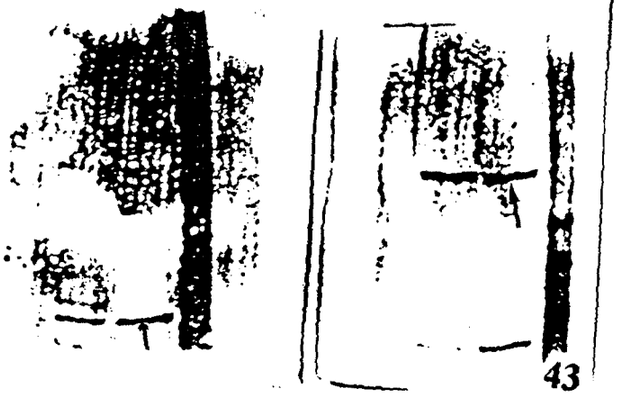

43

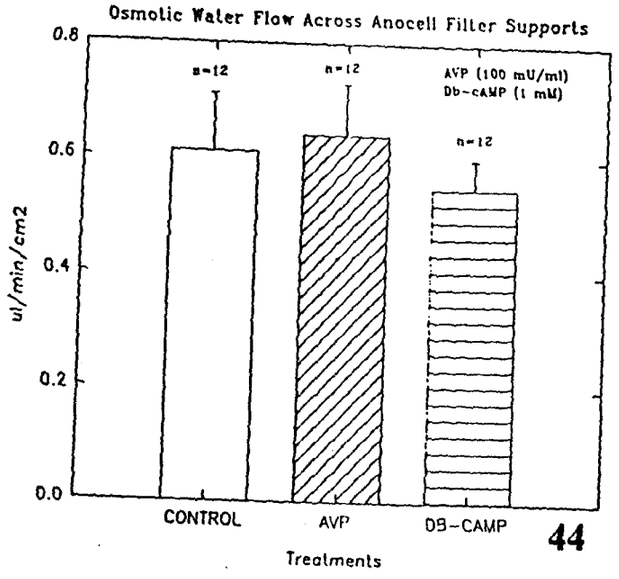

44

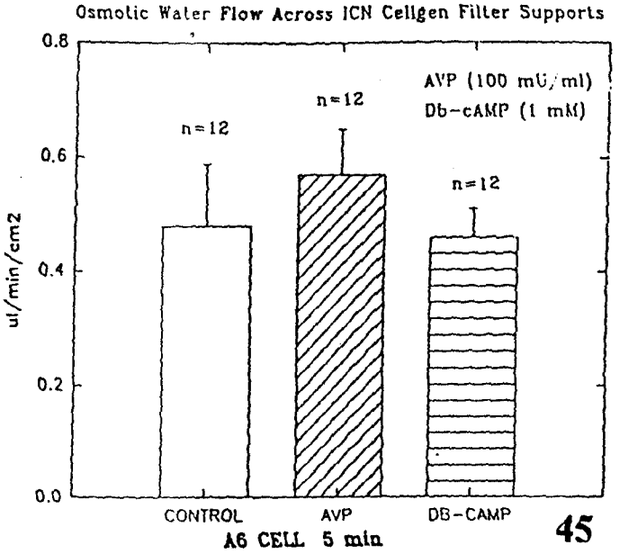

45

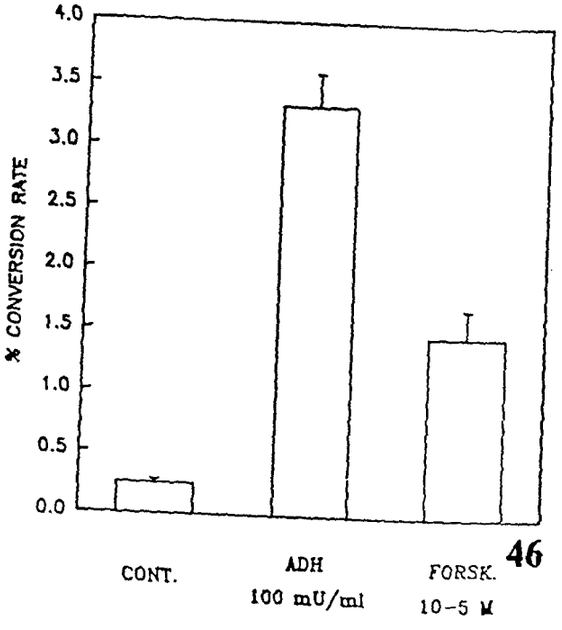

46

ADENYLCYCLASE ACTIVITY AS MEASURED BY AN ADENINE

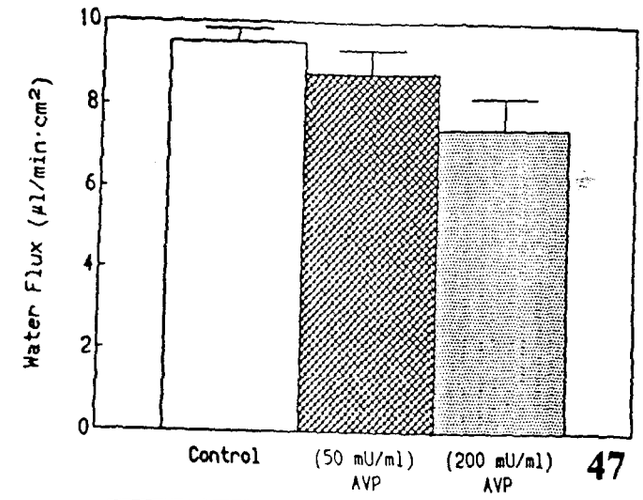
Water Flux (µl/min·cm²)
10
8
6
4
2
0
Control
(50 mU/ml) AVP
(200 mU/ml) AVP

47

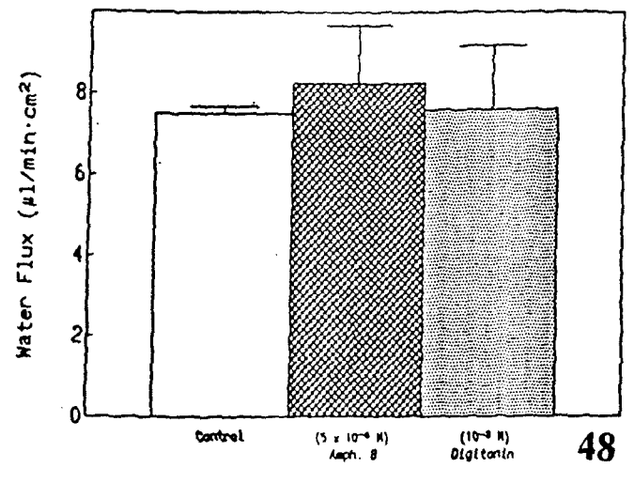
Water Flux (µl/min·cm²)
8
6
4
2
0
Control
(5 x 10⁻⁶ M) Aaph. B
(10⁻⁶ M) Digitonin

48

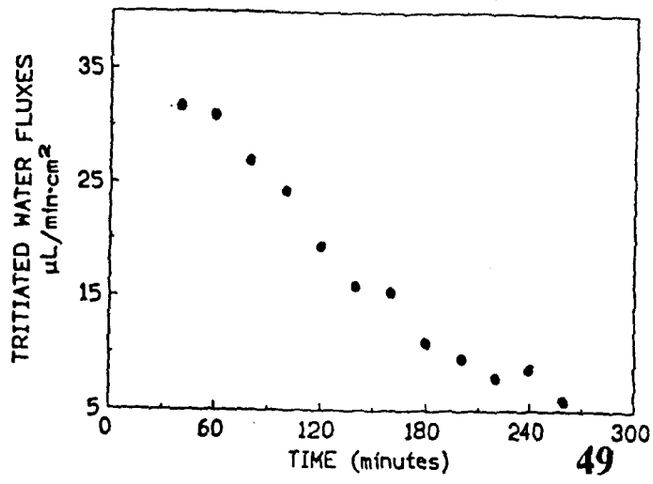
TRITIATED WATER FLUXES µL/min·cm²
35
25
15
5
0
60
120
180
240
300
TIME (minutes)

49

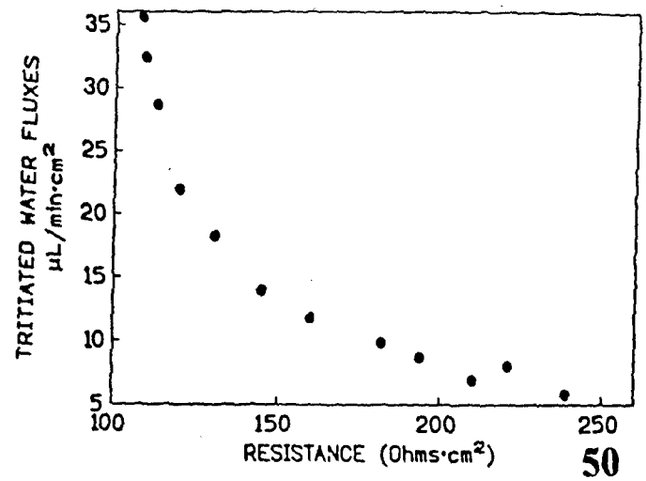
TRITIATED WATER FLUXES µL/min·cm²
35
30
25
20
15
10
5
100
150
200
250
RESISTANCE (Ohms·cm²)

50

TABLE 1. Electrical Properties of A6 Cells Grown on Anocell Filters			
TREATMENT	Potential Difference (PD- mV)	Short-Circuit Current (Isc- $\mu A/cm^2$)	Resistance (R-KΩ cm^2)
Control	37 ± 5	8 ± 1	4.6
ADH (10 min)	31 ± 4	11 ± 1*	2.7 *
AMILORIDE (30 min)	15 ± 3**	3 ± .6**	4.9**
AMPHOTERICIN B (30 min)	28 ± 3***	24 ± 4***	0.6***

The data represents the Mean ± S.E. of eight separate experiments.

*p<.05 from control.**p<.05 from ADH.***p<.05 from amiloride.

Figure 51

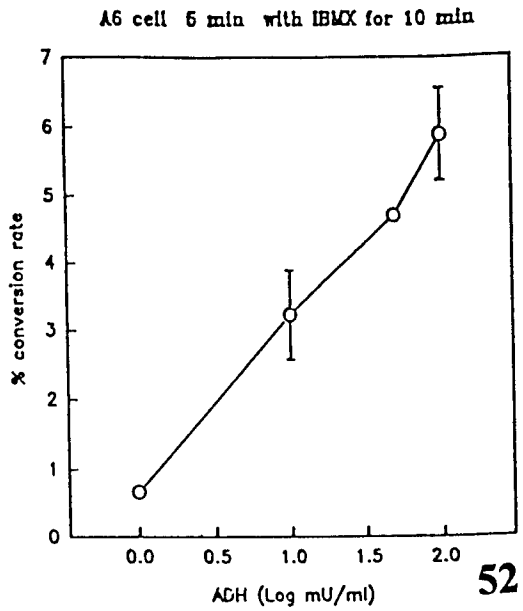
A6 cell 5 min with IBMX for 10 min
% conversion rate
0
1
2
3
4
5
6
7
0.0
0.5
1.0
1.5
2.0
ADH (Log mU/ml)

52

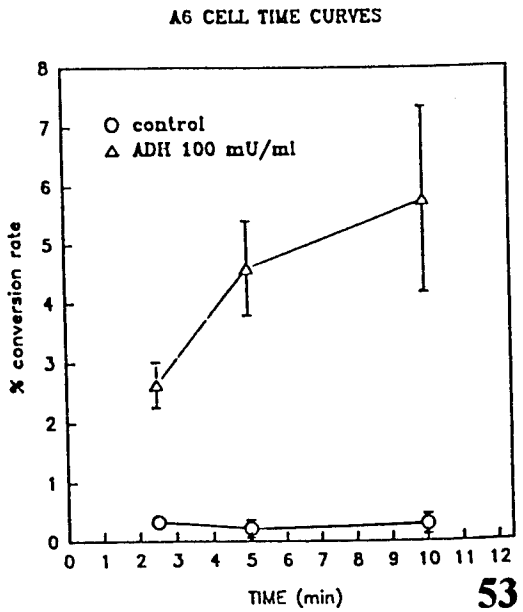
A6 CELL TIME CURVES
O control
Δ ADH 100 mU/ml
% conversion rate
0
1
2
3
4
5
6
7
8
0 1 2 3 4 5 6 7 8 9 10 11 12
TIME (min)

53


54

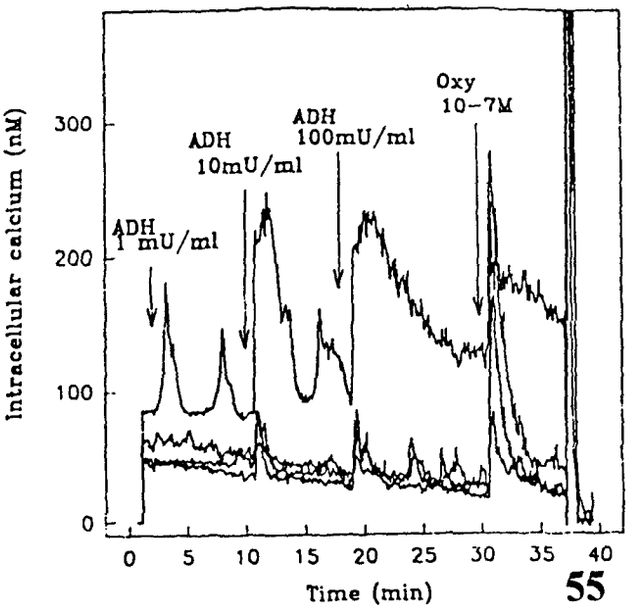

55

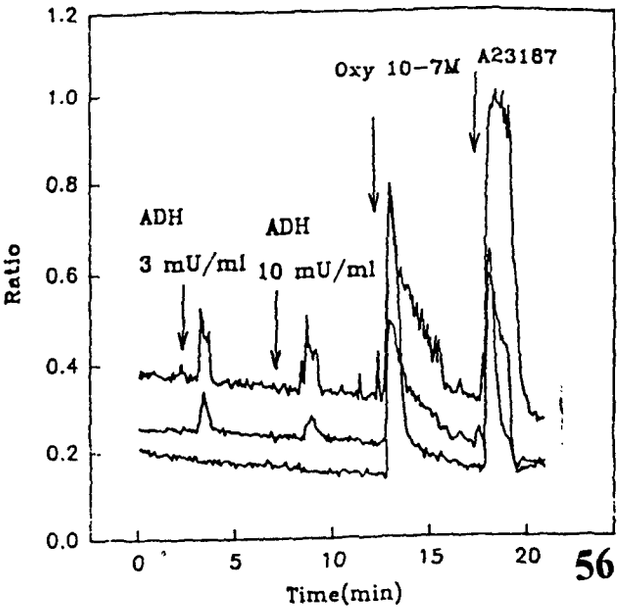

56

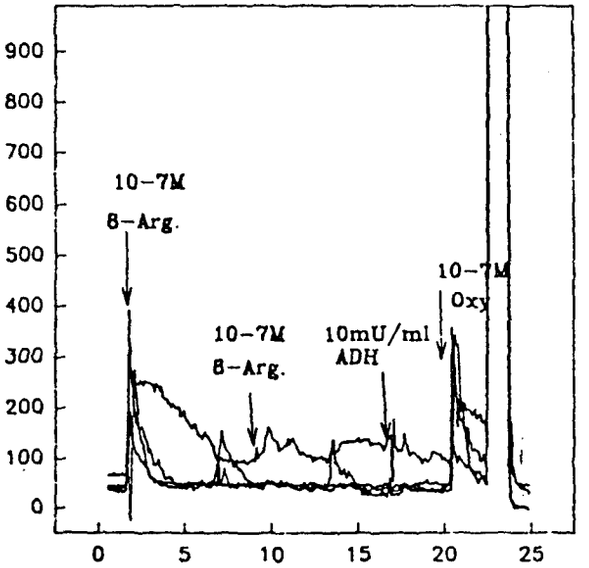

57

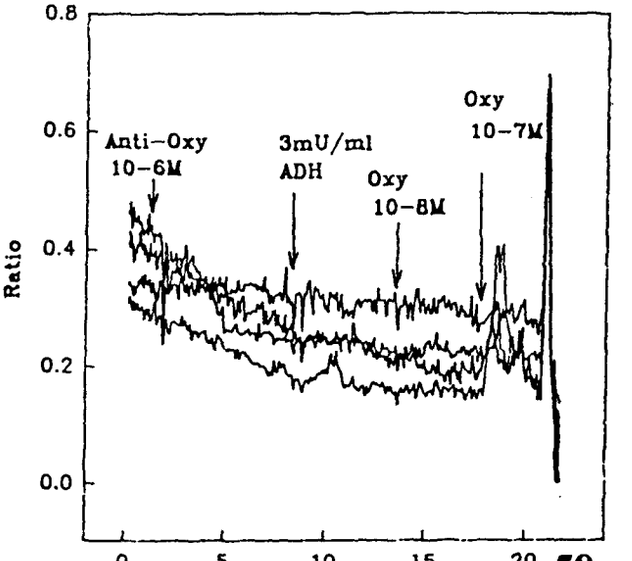

58

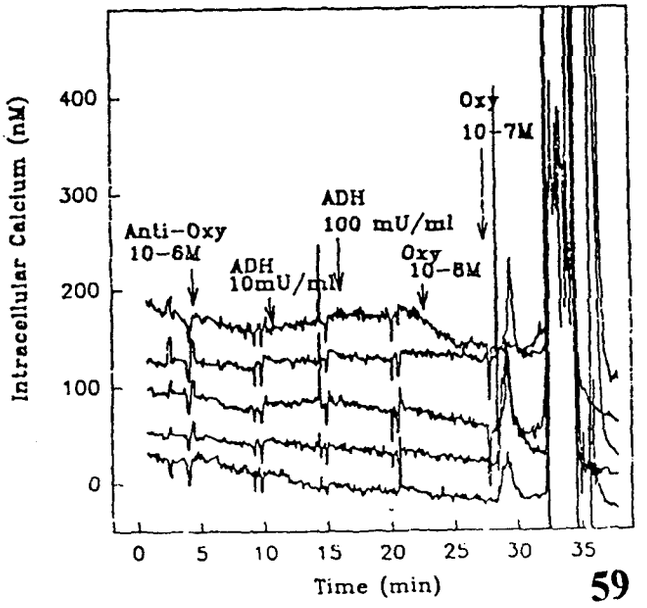

59

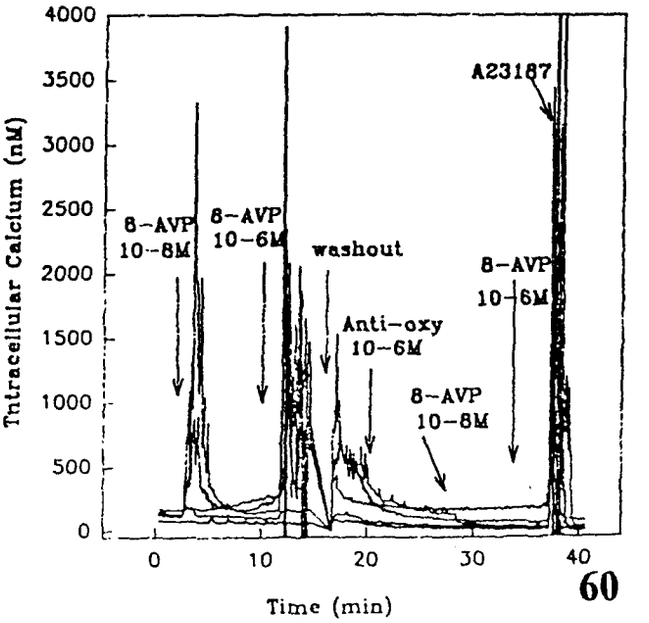

60

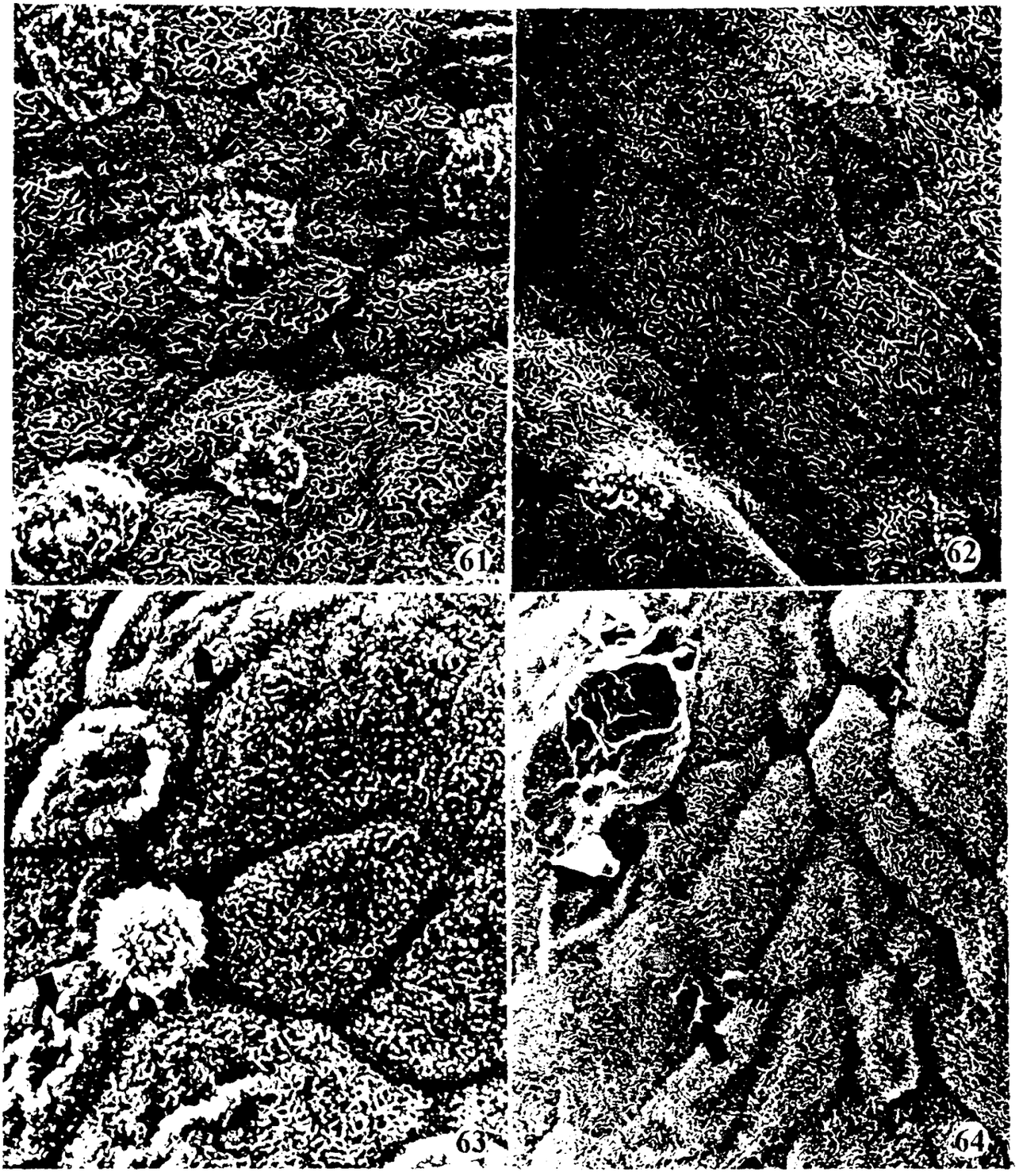
61
62
63
64

Graph Represents the Percentage of Endocytosed Cells Stimulated by ADH and MZ Compared to Control Tissues

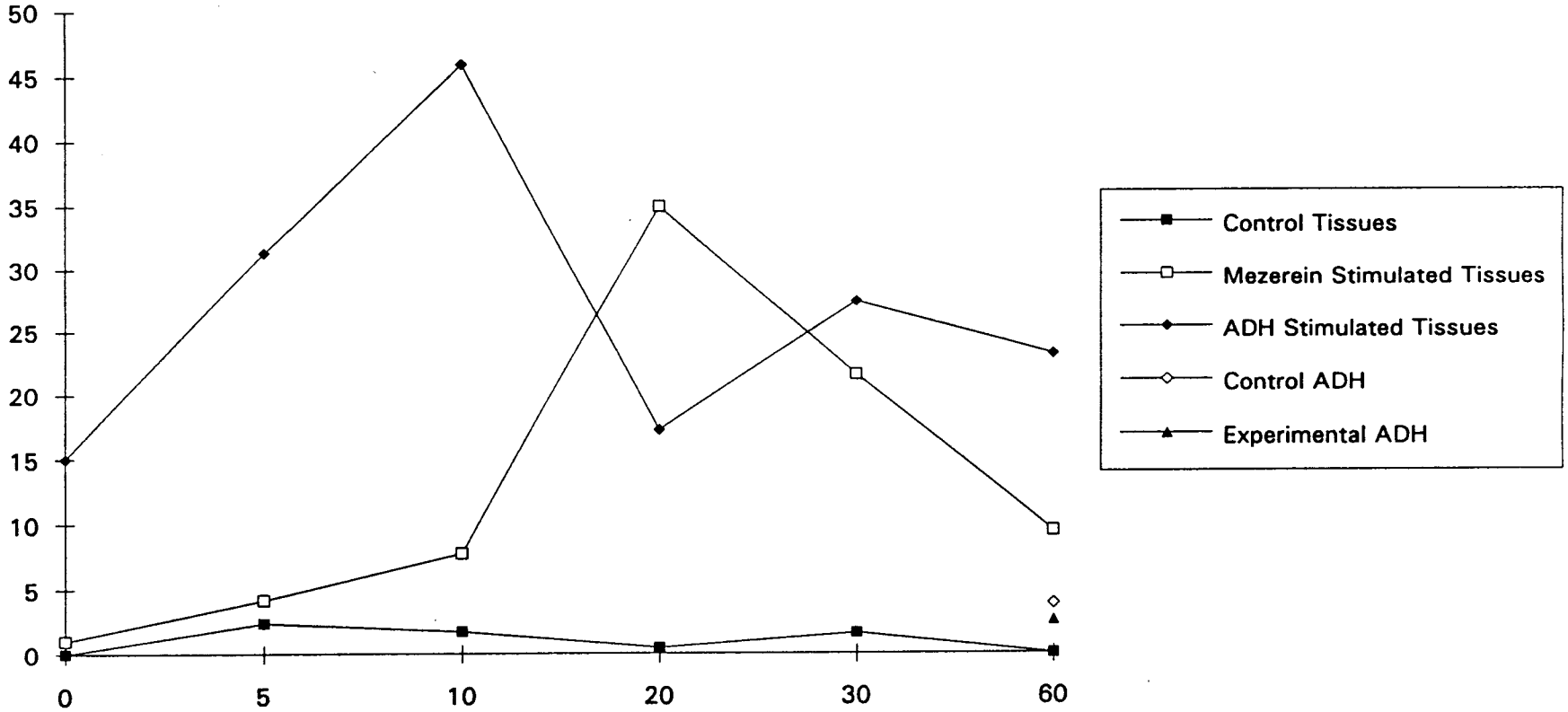

Figure 65


66


67


68

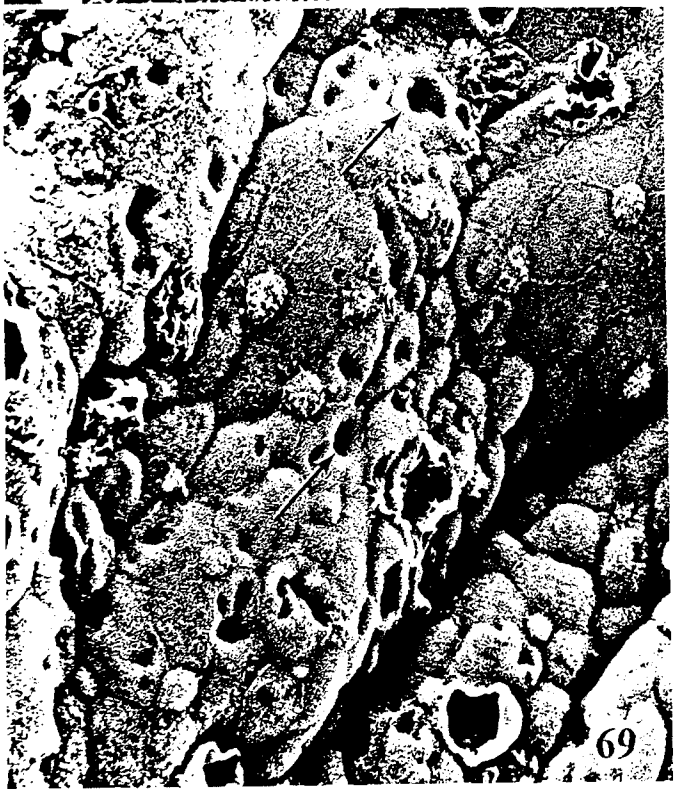
69


70


71


72


73

74

75

76

77

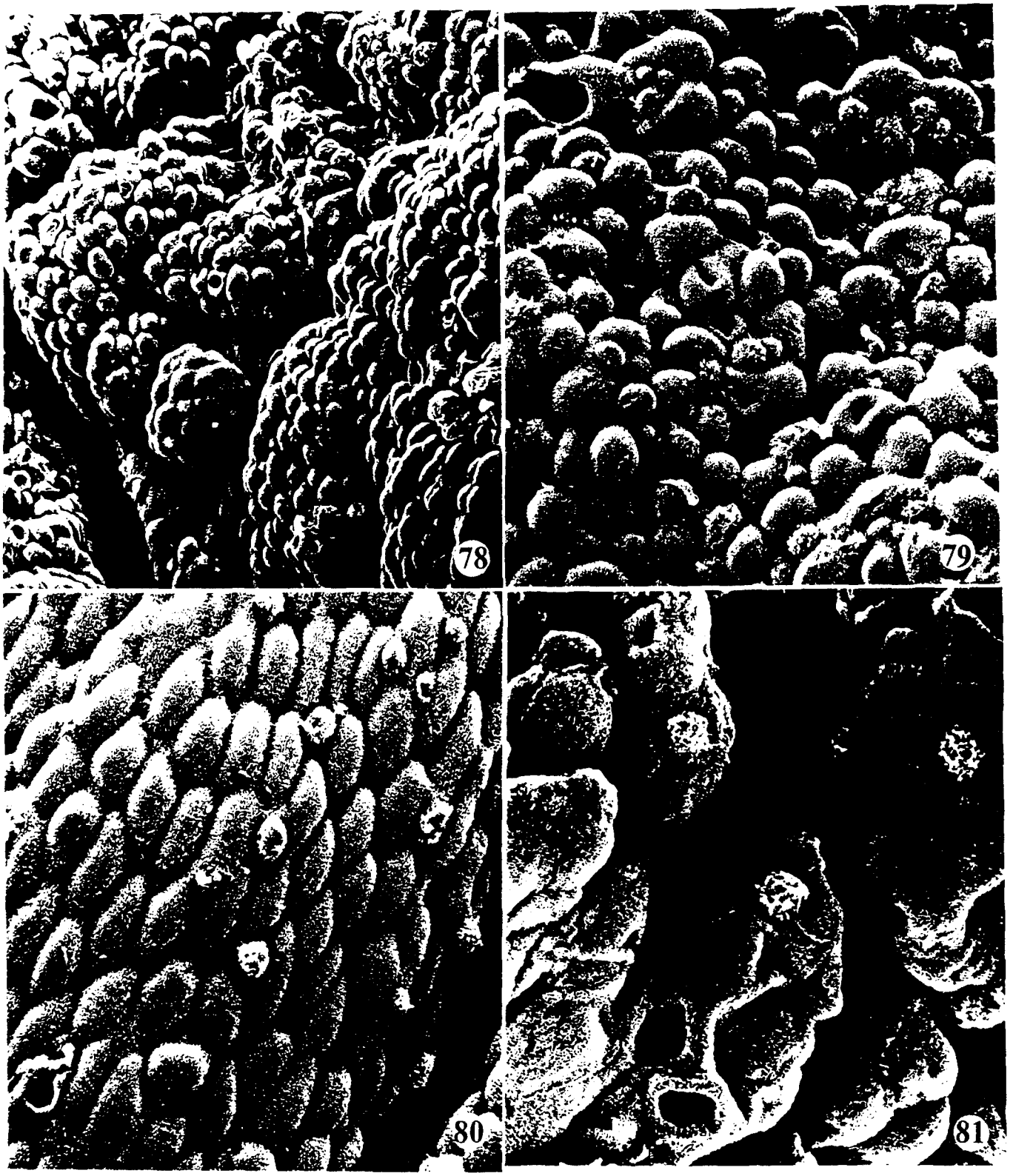
78
79
80
81


82

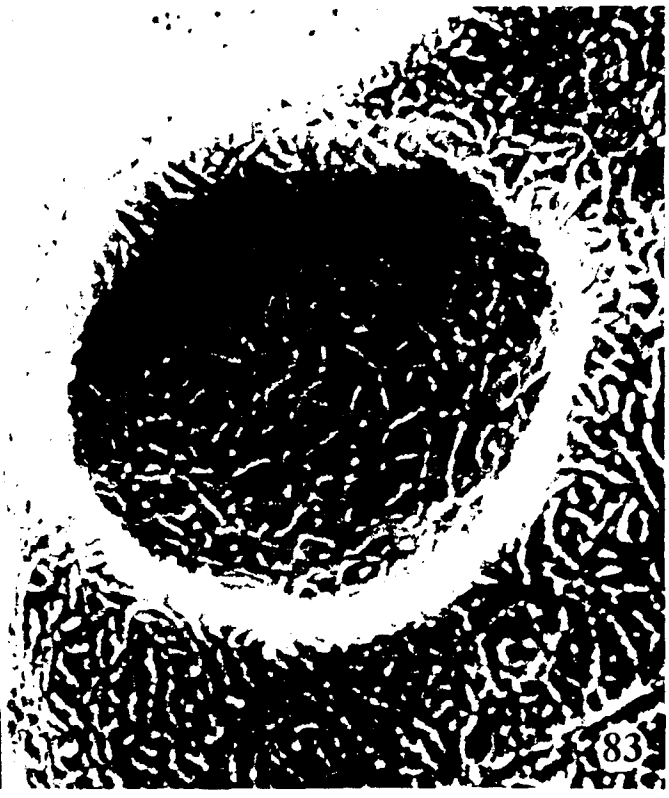
83

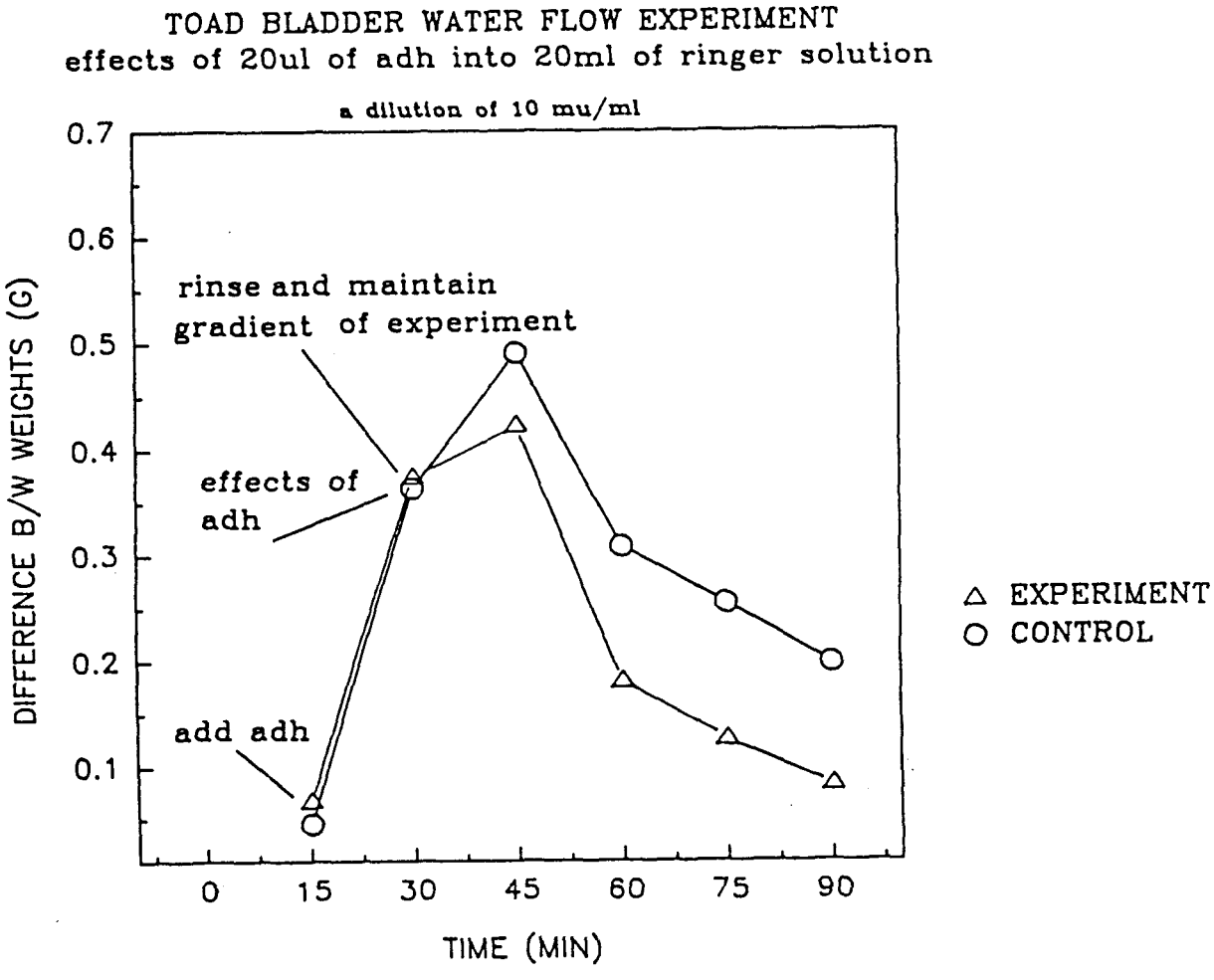
TOAD BLADDER WATER FLOW EXPERIMENT
effects of 20ul of adh into 20ml of ringer solution
a dilution of 10 mu/ml
DIFFERENCE B/W WEIGHTS (G)
0.7
0.6
0.5
0.4
0.3
0.2
0.1
rinse and maintain
gradient of experiment
effects of
adh
add adh
0
15
30
45
60
75
90
TIME (MIN)
△ EXPERIMENT
○ CONTROL

Figure 84